

1-1-2010

Metabolic Targeting Of Malignant Glioma: Modulation Of Glycolytic Flux By Erythropoietic Factors

Todd Brendon Francis
Wayne State University

Follow this and additional works at: http://digitalcommons.wayne.edu/oa_dissertations

 Part of the [Neuroscience and Neurobiology Commons](#)

Recommended Citation

Francis, Todd Brendon, "Metabolic Targeting Of Malignant Glioma: Modulation Of Glycolytic Flux By Erythropoietic Factors" (2010). *Wayne State University Dissertations*. Paper 87.

This Open Access Dissertation is brought to you for free and open access by DigitalCommons@WayneState. It has been accepted for inclusion in Wayne State University Dissertations by an authorized administrator of DigitalCommons@WayneState.

**METABOLIC TARGETING OF MALIGNANT GLIOMA: MODULATION OF
GLYCOLYTIC FLUX BY ERYTHROPOIETIC FACTORS**

by

TODD B. FRANCIS, M.D.

DISSERTATION

Submitted to the Graduate School

of Wayne State University,

Detroit, Michigan

in partial fulfillment of the requirements

for the degree of

DOCTOR OF PHILOSOPHY

2010

MAJOR: PHYSIOLOGY

Approved by:

Advisor

Date

© COPYRIGHT BY

TODD B. FRANCIS

2010

All Rights Reserved

DEDICATION

To my wife Amy for her undying love and support.

ACKNOWLEDGEMENTS

I am deeply indebted to Saroj Mathupala, Ph.D. for his never-ending patience, expert tutelage, and scientific prowess in support of my Ph.D. thesis. Without his support, this project would have not been possible. I would like to express my deepest gratitude to the neurosurgery department chairman & program director, Murali Guthikonda, M.D., who provided the financial & academic support for my research. I hope this project will help me represent his department with honor in my future academic endeavors. I would like to recognize Setti Rengachary, M.D., my original project co-advisor/mentor. I will never forget the overwhelming clinical & academic support throughout my career. His passing deeply saddened us all but the professional standards he set in the field of neurosurgery will be an undying example for future neurosurgical residents. I would also like to recognize Charlie Krafchak, Ph.D. who sadly and unexpectedly passed away before this work was completed. His help & support were invaluable and he will be sorely missed.

I would like to thank Drs: Blaine White, Donald De Gracia, Jonathon Sullivan, Brian O'Neil, and Gary Krause for providing me with such an invaluable solid foundation in basic science research. I would like to thank my committee members: James Rillema; Jose Rafols; Kenneth Casey; Sandeep Mittal; & Pat McAllister, for their support & leadership through this project. I am also deeply indebted to Ms. Christine Cupps for her expertise and never-ending (at times, saint-like) patience. Thank you also to Phil Benson; Michael Monterey; and Brandon Koch for their invaluable help in the lab.

Finally, I would like to thank my parents; Keith & Pat Francis, and my brother Scott for their support. Without them, I would not be where I am today.

TABLE OF CONTENTS

Dedication	ii
Acknowledgements	iii
List of Figures	vi
CHAPTER 1: GENERAL INTRODUCTION	1
Brain Tumors: Types, Grades, Incidence, Survival, Current Therapies	1
Metabolism of Glioblastoma vs. Normal Tissues	8
Monocarboxylate Transport	29
Preliminary Data	30
GATA Family of Transcription Factors	34
Project Outline and Hypothesis	37
Experimental Methodology	38
CHAPTER 2: EFFECT OF DOWN-REGULATION OF GATA-1 ON GLIOBLASTOMA SURVIVAL AND PROLIFERATION; AN <i>IN VITRO</i> STUDY	44
Introduction	44
Design of siRNA, Theory, and Transfection Methods: The mRNA Sequencing of GATA-1 and Location of siRNA Targets	45
Transient Transfection of Dharmacon siRNA into U87-MG	47
Long-Term Regulated Silencing of GATA-1: Tet-on/Tet-off System	49
SDS-PAGE and Western Blot for GATA-1 after Doxycycline and Minocycline Mediated Induction	55
Western Blot Analysis of both GATA-1 and MCT-2: Decrease in Levels of MCT-2 seen Concomitantly with Down-Regulation of GATA-1	58
MTT Assay for Cell Proliferation	60
CHAPTER 3: OVER-EXPRESSION OF GATA-1 IN GLIOBLASTOMA; AN <i>IN VITRO</i> STUDY	62

Introduction.....	62
Attempts to Over Express GATA-1 via Exposure of Glioma Cells to Erythropoietin (Epo).....	62
Overexpression of GATA-1 in U87-MG Cells via Transfection with a GATA-1 Expression Vector.....	63
MTT Assay for Cell Proliferation.....	65
Cell Cycle Analysis.....	66
Lactate Efflux by GATA-1 Overexpressing U87-MG.....	69
Luciferase Reporter Gene Analysis.....	71
CHAPTER 4: CONCLUSIONS AND FUTURE DIRECTIONS.....	76
GATA-1 Influences the Monocarboxylate Transporter-2 (MCT-2) Expression Resulting in Altered Glycolytic Capacity in GBM Cells.....	76
The Influence of GATA-1 on Tumor Growth has already been Acknowledged by the FDA.....	78
Future Directions.....	79
References.....	81
Abstract.....	88
Autobiographical Statement.....	90

LIST OF FIGURES

Figure 1: Glycolysis.....	9
Figure 2: Regulation of glycolytic enzymes.....	11
Figure 3: Glycolysis and Krebs cycle.....	12
Figure 4: Hexokinase in tumor cells.....	17
Figure 5: The citric acid cycle.....	22
Figure 6: The Cori cycle.....	23
Figure 7: Malignant tumors and their blood supply.....	24
Figure 8: The astrocyte-neuron lactate shuttle hypothesis.....	27
Figure 9: Upstream promoter of MCT-2 gene.....	31
Figure 10: Western blots of U-87MG homogenates for GATA-1.....	32
Figure 11: Western blots of surgical GBM specimens for GATA-1.....	33
Figure 12: 3-dimensional model of DNA binding domain of GATA-1.....	35
Figure 13: siRNA machinery schematic.....	40
Figure 14: shRNA sequence example.....	42
Figure 15: Inducible tTS (tet on/off) system of plasmids.....	43
Figure 16: Western blot of anti-GATA-1 siRNA treated U-87MG.....	49
Figure 17: Schematic of gene regulation in tTS (tet on/off) system.....	50
Figure 18: Regulatory and response shRNA plasmids.....	51
Figure 19: 0.8% agarose DNA gel of native plasmids.....	53
Figure 20: Western blot of doxycycline induction study.....	56
Figure 21: Quantification of doxycycline induction.....	56
Figure 22: Western blot of minocycline induction study.....	57

Figure 23: Quantification of minocycline induction.....	57
Figure 24: Western blot of double-probe study (GATA-1 and MCT-2).....	59
Figure 25: Densitometric analysis of double probe study (GATA band).....	59
Figure 26: Densitometric analysis of double probe study (MCT-2 band).....	60
Figure 27: Proliferation assay (MTT) of induced U-87MG.....	61
Figure 28: Schematic of GeneStorm GATA-1 expression vector.....	64
Figure 29: Western blot of GATA-1 overexpression in U-87MG.....	65
Figure 30: Proliferation assay (MTT) of GATA-1 overexpressed U-87MG.....	66
Figure 31: Diploid cell cycle analysis of U-87MG and negative control.....	67
Figure 32: Diploid cell cycle analysis of U-87MG test cells.....	68
Figure 33: Tetraploid cell cycle analysis of U-87MG and negative control.....	68
Figure 34: Tetraploid cell cycle analysis of U-87MG test cells.....	69
Figure 35: Schematic for enzymatic cycling assay.....	69
Figure 36: Enzymatic cycling assay absorbance spectrum.....	70
Figure 37: Lactate efflux rates in U-87MG and test cells.....	71
Figure 38: Reporter gene vector schematic.....	72
Figure 39: Reporter gene activation study.....	75
Figure 40: Epogen black box warning.....	79

CHAPTER ONE

GENERAL INTRODUCTION

Brain Tumors: Types, Grades, Incidence, Survival, and Current Therapies

The Human Brain - The human nervous system is broadly divided into the central nervous system (CNS) and the peripheral nervous system (PNS). The CNS is composed of the brain and spinal cord, whereas the PNS is the collection of spinal and cranial nerves that infiltrate all parts of the body, conveying messages to and from the CNS (Nolte and Sundsten, 2002). The CNS is covered by a tri-layered structure called the meninges, and is constantly bathed in cerebrospinal fluid (CSF) that is produced by the choroid plexus deep within the brain's ventricular system and reabsorbed by arachnoid granulations along the superior sagittal sinus.

Generally speaking, there are two major classes of cells in the human nervous system: neurons and glial cells; the latter provide a supporting function for the impulse transmission, structure, and the general function of the former. There are two major classes of glia in the vertebrate nervous system: microglia and macroglia. Microglia arise from macrophages outside of the nervous system and serve a phagocytic role. There are three types of macroglial cells: oligodendrocytes, Schwann cells, and astrocytes. Oligodendrocytes and Schwann cells myelinate axons of nerve cells thereby greatly increasing nerve conduction velocity along said axons; the former myelinate CNS neurons and the latter myelinate PNS neurons. Oligodendrocytes may myelinate the axons of several different neurons in their immediate vicinity, whereas Schwann cells only myelinate one axon. Astrocytes are the most numerous of all the glial cells, owing their name to their predominantly star-shaped cell bodies. Astrocytes

perform a wide range of roles in the nervous system including maintenance of the blood-brain barrier, mediation of extraneuronal ion concentrations and neuronal homeostasis, and to some extent (albeit indirectly) participation in cell signaling. Nerve cells, or neurons, are the main signaling units of the nervous system. A neuron has 4 morphologically defined regions: dendrites, a cell body, the axon, and presynaptic boutons. Dendrites serve to take in electrical information from other neurons in the form of post-synaptic potentials (these may be excitatory or inhibitory). At any given time all of these individual potentials combine to form one large potential (through, for example, “spatial” or “temporal” summation) which is then transmitted to the initial segment of the neuronal axon (the “axon hillock). If this potential is of sufficient strength, it will trigger depolarization of the axon hillock and initiate a nerve impulse down the axon into the presynaptic terminals where this electrical energy is converted to chemical energy through the voltage-dependent release of synaptic vesicles containing neurotransmitters. These neurotransmitters are released into the synaptic cleft (separating the presynaptic terminals of one neuron from the postsynaptic receptors of another) and can have a variety of effects on the next neuron (Kandel et al., 2000).

Tumors of the PNS or CNS can arise from virtually any of the aforementioned brain structures. For example, there are tumors of the meninges (termed “meningiomas”), tumors of the peripheral nerves and associated glial cells (Schwannomas, neurofibromas, and the like), tumors of the nerves themselves (“gangliocytomas”, “neurocytomas”), and tumors of the glial cells (astrocytomas, oligodendrogliomas, etc.). It is these tumors of the glial cells that is the central focus of my research; in particular one of the most severe forms of astrocytoma in existence

(glioblastoma).

Classification of Brain Tumors - The revised WHO Histological Typing of Tumors of the Central Nervous System (Louis and International Agency for Research on Cancer., 2007) classifies astrocytic tumors as tumors of neuroepithelial tissue. Tumors of neuroepithelial tissue are subdivided into nine categories: astrocytic, oligodendroglial, ependymal, mixed glial, choroid plexus tumors, neuroepithelial tumors of uncertain histogenesis, neuronal and mixed neuronal-glial tumor, pineal tumor, and embryonal tumor. Astrocytic tumors, in turn, are subdivided into six groups: diffuse astrocytoma, anaplastic astrocytoma, glioblastoma, pilocytic astrocytoma, pleomorphic xanthoastrocytoma, and subependymal giant cell astrocytoma.

The WHO also classifies tumors of cranial and paraspinal nerves, including Schwannoma, neurofibroma, perineuroma, and malignant peripheral nerve sheath tumor (MPNST). Also classified by the WHO are tumors of the meninges (meningothelial cell tumors, mesenchymal tumors, primary melanocytic lesions, and other), and lymphomas, germ cell tumors, sellar region tumors, and metastatic lesions.

Tumor Grading - The WHO has implemented a grading scheme for CNS tumors that serves as a “malignancy scale” in order to evaluate these tumors. For a given CNS tumor there are 4 WHO grades possible, simply classified as WHO grade I, II, III, or IV. WHO grade I lesions generally include tumors with low proliferative potential and possibility of cure with surgical resection alone. There are only 2 astrocytic tumors that fit this grade: subependymal giant cell astrocytoma (SEGA) and pilocytic astrocytoma. Other examples (to name a few) of WHO grade I tumors include meningioma, subependymoma, and choroid plexus papilloma. WHO grade II tumors are generally

infiltrative in nature and tend to recur despite gross total surgical resection. These lesions also tend to progress to higher grades of malignancy. Examples of WHO grade II tumors include diffuse astrocytoma, oligodendroglioma, ependymoma, atypical meningioma, and hemangiopericytoma. A tumor that has earned the grade of WHO grade III exhibits histological evidence of malignancy (specifically nuclear atypia and abundant mitotic figures). Anaplastic astrocytoma, anaplastic oligodendroglioma, and anaplastic meningioma are all examples of WHO grade III lesions. WHO grade IV lesions are cytologically malignant, mitotically active, necrotic neoplasms usually associated with rapid progression of disease and poor outcome. Medulloblastoma, glioblastoma, and pineoblastoma are all examples of WHO grade IV tumors (Louis and International Agency for Research on Cancer., 2007).

With the aforementioned exceptions of SEGA and pilocytic astrocytoma, the grading of astrocytic tumors are graded in a 3 tiered system based on their histology. Tumors with cellular atypia alone are WHO grade II (diffuse astrocytoma); tumors also showing anaplasia and mitotic activity are WHO grade III (anaplastic astrocytoma), and tumors additionally showing necrosis and/or microvascular proliferation are WHO grade IV. There are 3 astrocytic tumors that are WHO grade IV lesions: glioblastoma, gliosarcoma, and giant cell glioblastoma (Louis and International Agency for Research on Cancer., 2007). Glioblastoma is characterized microscopically by necrosis and/or endothelial cell proliferation coupled with increased cellularity, mitotic figures and pleomorphism (Kaye and Laws, 2001; Kleihues and Sobin, 2000).

Epidemiology of Primary Brain Tumors - The incidence of primary malignant or benign brain tumors in the United States is 18.71/100,000 person-years; while

7.19/100,000 are diagnosed with a malignant brain tumor, 11.52/100,000 are non-malignant. There are about 13,000 deaths annually from these tumors, placing brain malignancies among the top 10 leading causes of cancer-related deaths. 4.71/100,000 children will have a primary brain tumor before age 20 years. The distribution of primary brain tumors in the general population is strongly age specific. The incidence rates are higher in pediatric males (4.75/100,000 male vs. 4.66/100,000 female) and in adult females (19.88/100,000 female vs. 17.44/100,000 male). The incidence rate of primary malignant brain tumors, however, is higher in males than in females (7.6/100,000 male vs. 5.4/100,000 female) (Wrensch et al., 2002). Gliomas and other neuro-epithelial tumors constitute 49% of primary brain tumors, while meningiomas are the second most common type (27%). Specifically looking at histology, meningioma is the most common type at 33.8%, followed by glioblastoma (17.1%) and pituitary (12.7%) (Wrensch et al., 2002).

The probability of histological malignancy in an astrocytoma is 0.34 between 30-34 years and 0.85 after the age of 60. The incidence of glioblastoma and astrocytoma per 100,000 population rises from 0.2 and 0.5 in the under-age 14 group to 4.5 and 1.7 (respectively) after the age of 45. Along with the age-related shift in histology we also see a shift in location: Under the age of 25 years, 67% of astrocytomas are infratentorial (in other words, in the brainstem or cerebellum) whereas over the age of 25 years 90% are supratentorial (in the cerebral cortex, basal ganglia, diencephalon, deep white matter, etc.). The terms “supratentorial” and “infratentorial” refer to the “tentorium”: a leaflet of dura separating the cerebellum from the cerebral cortex. In the USA, glioblastoma occurs at the greatest mean age of all brain tumors (60.2 years). In most

series there is a slight preponderance of males observed for glioblastoma incidence (Kaye and Laws, 2001).

Survival - The 5 year relative survival rate of a primary brain tumor is 33.6% in males and 37% for females. Broken down by age, 5 year relative survival rates are as follows: 0-19 years = 72.1%, 20-44 years = 55.9%, 45-54 years = 30.7%, 55-64 years = 16.7%, 65-74 years = 9.6%, and age 75 or older = 5.2% (CBTRUS data: <http://www.cbtrus.org/2007-2008/2007-20081.html>). Survival rate is closely tied in with tumor histology, and glioblastoma has one of the worst 5-year survival rates of all the brain tumors. To illustrate: 5-year survival rates for pilocytic astrocytoma = 94%, for oligodendroglioma = 79%, for anaplastic oligodendroglioma = 47%, and for anaplastic astrocytoma = 27%. The 5-year survival rate for glioblastoma = 4.46%.

Glioblastoma - Glioblastoma is the most common, and unfortunately the most deadly, malignant primary brain tumor. Current medical and surgical therapies only minimally prolong life expectancy and improve quality of life and are generally ineffective at specifically addressing the underlying pathology. The primary reason for this is that by the time patients present with a Glioblastoma, the tumor has already microscopically spread to other areas of the brain outside of the grossly obvious tumor location. Successful treatment of Glioblastoma must therefore directly address unique characteristics of the individual tumor cell on a molecular level as well as the macroscopic elements of the tumor. Effective treatment of Glioblastoma will most likely be a combination of surgical intervention directed at grossly reducing the size of the tumor itself (gross tumor debulking, BCNU implantation, radiotherapy and radiosurgery, etc.) and molecular techniques that target the tumor cells individually (vaccines and

immunotherapy, viral vectors and gene therapy, etc.).

Current Therapies for Glioblastoma - The current standard-of-care for operable glioblastoma includes surgical resection followed by radiation and chemotherapy (Sathornsumetee et al., 2007). Several factors determine whether a glioblastoma is operable or inoperable. In general, if the tumor is of the “butterfly” type (i.e. invading the corpus callosum and both hemispheres) or infiltrating the deep brain structures (hypothalamus, basal ganglia, etc.), then the tumor is usually deemed inoperable. Once the diagnosis of glioblastoma has been established, a craniotomy and extensive tumor debulking surgery should be performed with the goal of removing as much tumor as surgically possible while maintaining the integrity of the surrounding and intervening structures that are absent of any gross tumor invasion. Gross total or near-total resection has been shown to increase survival (Cavaliere et al., 2007) significantly (Lacroix et al., 2001). As an adjunct, post-surgical radiation therapy is administered in 1.5 to 2 Gy fractions to a total dose of 58 to 60 Gy to the tumor bed or resection cavity with a 2-3 cm margin (Sathornsumetee et al., 2007). There are several chemotherapeutic agents used as adjuvant therapy in GBM. Nitrosoureas such as carmustine/BCNU are lipophilic agents that readily cross the blood-brain barrier and form cross-links in DNA. BCNU-impregnated wafers (Gliadel) may be implanted in the resection cavity after gross total GBM resection. BCNU has been shown to increase eighteen month survival, but not median survival, in patients status-post GBM resection (Cavaliere et al., 2007). Temozolomide (Temodar) is an oral methylating agent with near 100% bioavailability. Temozolomide methylates DNA at the O6 position of guanine which results in base pair mismatch during replication. Clinicians had high

hopes for temozolomide use in conjunction with radiation therapy for GBM patients, however median survival increase has been shown to be modest (14.6 months vs. 12.1 months) (Robins et al., 2007). Irinotecan is a water soluble camptothecin derivative that inhibits topoisomerase I, preventing re-ligation of DNA following single strand breaks. It has been studied extensively in patients with recurrent GBM and in combination with other agents such as BCNU and temozolomide. Irinotecan has been shown to potentiate the activity of both BCNU and temozolomide when administered in combination (Cavaliere et al., 2007). Bevacizumab (Avastin) is a monoclonal Ig(G) antibody that binds to and inhibits human VEGF-A. It has shown some promise in GBM patients, especially in combination with irinotecan (Cavaliere et al., 2007).

As stated in the introduction, the aforementioned conventional management of patients with glioblastoma is generally unsatisfactory because an algorithmic treatment plan cannot deal with the extreme cellular heterogeneity and therapeutic resistance of the tumor. None of the above adjunctive or adjuvant treatments has been shown to significantly increase median survival of GBM patients. Future treatment plans must be tailored to adapt to the wide diversity of cells in a solid glioblastoma as well as associated micrometastases (Kaye and Laws, 2001).

Metabolism of Glioblastoma vs. Normal Brain

Normal Brain Metabolism - The brain is a unique organ in that it relies solely on glucose (and ketone bodies in case of starvation) for energy. It keeps no glycogen or fat storage, and so in essence is an “end organ” with regards to substrate. Since the brain relies solely upon blood glucose, substrate supply is thus a function of cerebral blood flow (Kaye and Laws, 2001).

Under normal circumstances, average human cerebral blood flow is 45 to 60 ml/100 grams of brain/minute, representing roughly 15% of cardiac output. Flow is maintained across a wide range of perfusion pressures by the process of autoregulation, allowing adequate substrate delivery (O₂ and glucose, predominately) to meet metabolic demands. The normal cerebral metabolic rate of oxygen is approximately 3.5 ml/100 grams of tissue/min (20% of resting total body O₂ consumption). The majority of this oxygen is used by the normal brain to generate energy through the aerobic metabolism of glucose (Zauner et al., 2002).

The first step in the cellular metabolism of glucose is the process of glycolysis (Figure 1). Glucose is transported from the bloodstream into the brain by carrier-mediated transport across the blood-brain barrier by the GLUT-1 transporter and then into neurons by the GLUT-3 transporter (GLUT-1 in astrocytes).

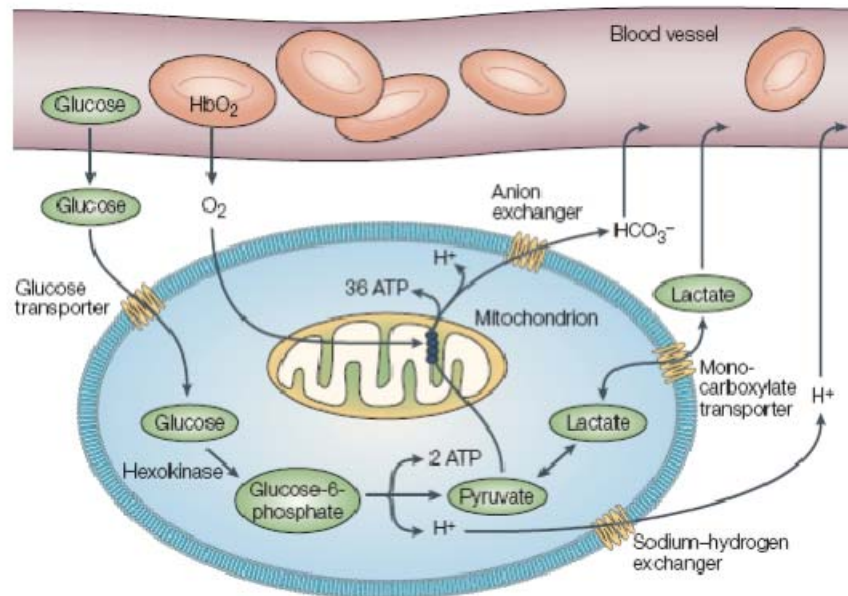


Figure 1: Excess hydrogen ions as by-products of metabolic processes are shunted out of the cytosol by lactate transporters and other ion exchange proteins in the cell membrane (Gatenby and Gillies 2004).

Once inside of the cell, D-glucose is phosphorylated by the enzyme hexokinase (HK) to glucose 6-phosphate. HK has a low K_m (and therefore a high affinity) for D-glucose, allowing for efficient metabolism of glucose even in low tissue quantities. HK is down-regulated by its metabolic product, glucose 6-phosphate, as well as increased ATP/ADP ratios (which essentially are one in the same, since the metabolic intermediates of glycolysis like glucose 6-phosphate will accumulate in the cell if energy stores are high and downstream metabolic processes slow down). The rate-limiting enzyme of glycolysis is phosphofructokinase-1 [PFK-1], which is activated by intracellular AMP levels (an indicator of increased ATP usage). It catalyzes the irreversible phosphorylation of fructose 6-phosphate to fructose 1,6-bisphosphate. ATP and citrate (indicators of high amounts of energy stores) are allosteric inhibitors of PFK-1 (Mangiardi and Yodice, 1990). The final step in glycolysis is also the final regulatory step, and it is catalyzed by pyruvate kinase (PK). PK converts phosphoenolpyruvate to pyruvate. Fructose 1,6-bisphosphate is a strong activator of PK (feed-forward regulation effectively links the kinase activities of PFK-1 and PK) (Figure 2).

Under normal circumstances, the pyruvate that is generated by glycolysis is then shunted into the Citric Acid Cycle [TCA cycle or Krebs Cycle]. Pyruvate that is not used in the TCA cycle is reduced by lactate dehydrogenase and NADH to form lactate (anaerobic glycolysis) or converted into the amino acid alanine. Pyruvate then enters the mitochondria where it can enter the TCA cycle as either acetyl coenzyme A (main path) or oxaloacetate.

In the TCA cycle, acetyl coenzyme A and oxaloacetate are metabolized to form NADH and FADH₂ which then enter the electron transport chain [ETS] to generate ATP.

The TCA cycle is also regulated in response to metabolic demands; its rate limiting

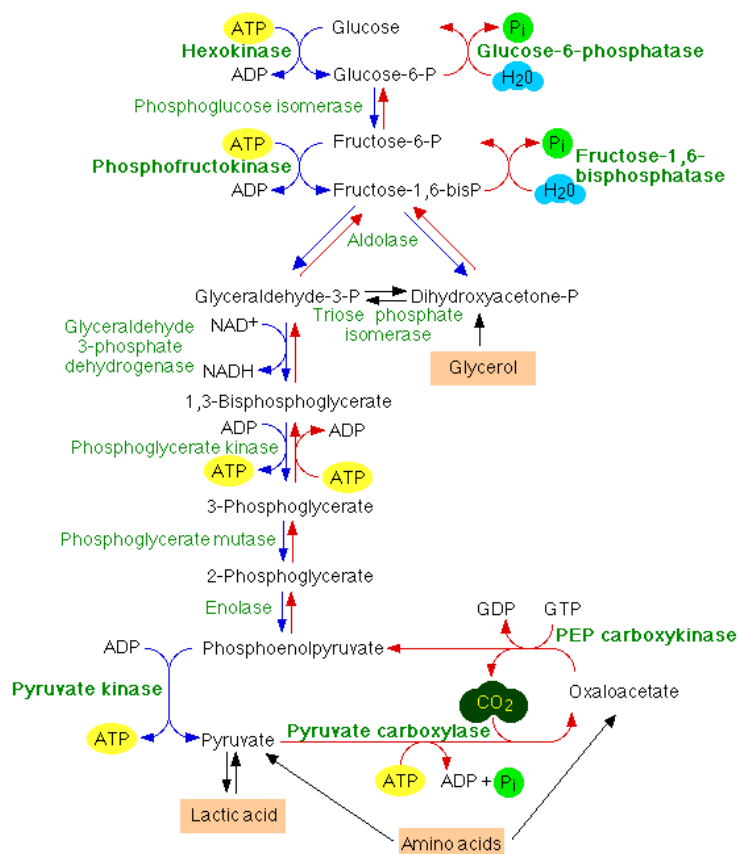


Figure 2: In normal cells, glycolysis is regulated at 3 steps (PFK-1, HK, PK). In malignant tumor cells, these enzymes fail to respond to normal metabolic signals and are constitutively activated, leading to uncontrolled lactate production. (<http://138.192.68.68/bio/Courses/biochem2/Gluconeogenesis/GluconeogenesisResources/GlycolysisGlucoNeo.gif>)

enzyme is isocitrate dehydrogenase which is activated by ADP and inhibited by NADH. (Berg et al., 2006; Zauner et al., 2002) (Figure 3). According to the chemiosmotic hypothesis, the mitochondria use electrons donated by NADH and FADH₂ to pump hydrogen ions across inner mitochondrial (hydrogen ion-impermeable) membrane into the intermembrane space of the mitochondrion using a series of transport proteins. The electron is passed from complex I to III and IV, creating a hydrogen ion gradient across the inner mitochondrial membrane. When the electron reaches complex IV (cytochrome

oxidase), the electron is donated to O_2 giving H_2O . Complex V (F₀/F₁-ATP synthase) then uses the ion gradient to generate ATP from ADP and Pi. The net (theoretical) yield of this process of oxidative phosphorylation is 38 ATP, 6 CO₂, and 6 H₂O per 1 mole of glucose (Zauner et al., 2002) although in practice approximately 30 ATP are made due to proton leakage across the inner-mitochondrial membrane (Berg et al., 2006).

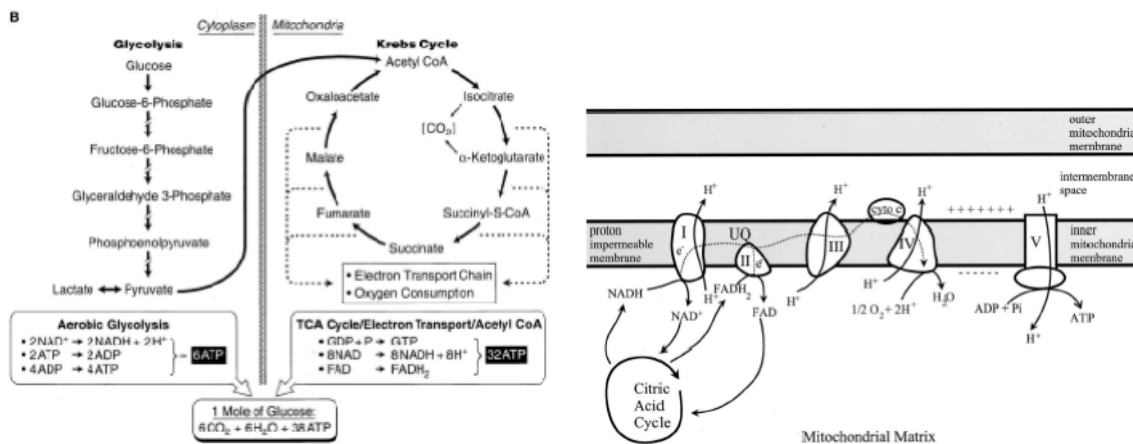


Figure 3: Glycolysis takes place in the cytosol of mammalian cells, while the Krebs cycle and the electron transport chain take place in the mitochondria (Zauner, Daugherty et al. 2002).

In mammalian cells, glycolysis is inhibited by the presence of oxygen, which allows mitochondria to fully oxidize pyruvate to CO₂ and H₂O. This inhibition is referred to as “the Pasteur effect” after Louis Pasteur who was the first to demonstrate that glucose flux was reduced by the presence of oxygen (Gatenby and Gillies, 2004). However, even since the early 1920’s researchers like Otto Warburg had observed that many tumor cells metabolized glucose in a very different way. Modern positron-emission tomography (PET) using fluorodeoxyglucose (FdG) has shown that most primary and metastatic tumors show significantly increased glucose uptake as compared to normal cells, a so-called “glycolytic phenotype” (Gatenby and Gillies, 2004; Pedersen, 1978). This phenotype seems to manifest itself through up-regulated

glucose transport into malignant cells (via up-regulation of GLUT-1 and GLUT-3 glucose transporters on the cell surface) and an up-regulated phosphorylation step (Glucose to glucose-6-phosphate, catalyzed by hexokinase). Tumor cells have been shown to maintain this glycolytic phenotype in culture under normoxic conditions, and the rate of glycolysis in cultured cell lines seems to linearly correlate with tumor aggressiveness (Gatenby and Gillies, 2004). Furthermore, it appears that many malignant cell lines exhibit what is known as the “Crabtree effect”: In the presence of glucose, oxygen consumption in tumor cells is impaired (in essence, the opposite of the Pasteur effect) (Argiles and Lopez-Soriano, 1990).

Metabolism of the Malignant Astrocytoma - The term *anaplasia* refers to a process of malignant change which may occur in any tissue type. The process of anaplasia includes several survival mechanisms that allow a neoplasm to compete successfully with its host. These include:

1. Utilization of primitive enzyme systems that give the tumor energy management and growth advantages over the host
2. Tumor vs. host products such as tissue lytic enzymes, immune-suppressors, growth factors, etc.
3. Extracellular matrix modifications including pH, oxygen tension level alteration, and perfusion change
4. Cell membrane alterations including antigenic mutation, second messenger enhancements
5. Autoinduction (A process by which a tumor cell virtually guarantees its own unrestrained growth and replication)

The above mechanisms allow malignant brain tumors to gain a survival advantage over their hosts and replicate beyond the control of the host immune system. This certainly puts the host at a clear disadvantage when attempting to combat a brain tumor, however because many of these processes are unique to tumor cells they offer significant targets for potential antitumor therapies (Kaye and Laws, 2001).

Since the 1930s there has been a great deal of research comparing the metabolism of malignant astrocytes to that of normal astrocytes. As I will presently explain, this research has shown that the metabolic processes of malignant astrocytes are much different from those of normal cells, and this difference is thought to augment the malignant cell's chance for survival in an otherwise normal host environment.

Every cellular metabolic process can be traced back to genetic information stored in a cell's DNA. The information encoded on DNA is copied to messenger RNA [mRNA] and are then exported from the nucleus to the cytosolic rough endoplasmic reticulum where it is *translated* into proteins by the ribosomes. The most crucial proteins are the enzymes since they are responsible for the production of the metabolic and structural machinery of the cell. In neoplastic cells, changes have occurred to allow for the introduction of a new genetic code into the cellular DNA, duplication and amplification of existing portions of the code, and/or the unmasking of normally repressed genes in the code. Certain genes in the code are referred to as *proto-oncogenes* in that they are normal portions of the genetic code that control cell proliferation, maturation and differentiation. Once these genes are activated, they become *oncogenes* and can result in the neoplastic transformation of a normal cell through the action of the peptide that it codes. Processes that convert proto-oncogenes into oncogenes include gene mutation,

amplification, and translocation or rearrangement. Expression of genes that were previously silent can lead to the presence of an entirely different set of metabolic machinery in cancer cells that can, in part, explain their strange behavior when compared to normal cells. Indeed, researchers have recently discovered a molecule called *hypoxia inducible factor-1 alpha* (HIF-1). HIF-1 is widely overexpressed across a broad range of cancers and is thought to control cellular and systemic responses to oxygen availability and coordinates up-regulation of genes involved in many pathways concerned with tumor growth and metabolism, cellular proliferation, differentiation and viability, apoptosis, pH regulation, and matrix metabolism (Stubbs et al., 2003). Specifically, it induces survival genes such as glucose transporters, angiogenic growth factors (for example, vascular endothelial growth factor [VEGF]), hexokinase II, and hematopoietic factors (for example, transferrin and erythropoietin [EPO]) (Gatenby and Gillies, 2004). Interestingly, a mutation in the von Hippel-Lindau (VHL) ubiquitin ligase produces constitutively high expression of HIF-1, as the wild type protein marks HIF-2 for proteasomal degradation. Re-insertion of transgenic VHL restores normal levels of HIF-1 and (not coincidentally) greatly reduces aerobic glucose consumption rates. Although significant, hypoxia is not the only factor that can stabilize HIF-1 in tumor cells. Other examples include cyclooxygenases, heat shock proteins, insulin-like growth factors, and thioredoxin (Gatenby and Gillies, 2004). This may help explain how malignant tumor cells have such a different pattern of metabolism than normal host cells, for example, constitutive up-regulation of glycolysis is likely to be (in part) an adaptation to hypoxia that develops as pre-malignant lesions grow progressively further from their blood supply (Gatenby and Gillies, 2004). This is unlikely to be solely a result

of hypoxia, since this malignant phenotype of up-regulated glycolysis is seen in normoxic conditions in tumor cells and rapidly dividing host cells. Many researchers feel, however, that this glycolytic phenotype is necessary for malignant tumor evolution and invasion.

Tumors, especially malignant tumors, were once thought to rely solely on glucose and/or glutamine for metabolic fuel. It wasn't until recently that researchers began to realize that tumor cells may draw upon a wide range of fuels, for example fatty acids, amino acids (other than glutamine), and ketone bodies. In fact, when MCF-7 breast cancer cells were examined in culture, researchers found that glucose and glutamine were significant fuels but only accounted for less than half of total ATP turnover (Guppy et al., 2002).

Aerobic Glycolysis - The mean ATP and total adenylate levels in astrocytic tumors have been shown to be significantly higher than in surrounding brain. This is explained logically by the fact that malignant astrocytomas have to satisfy both basic metabolic demands and tumor growth. As previously described, normal cells prefer to utilize oxygen to fully metabolize glucose using oxidative phosphorylation, but in situations where O_2 is in short supply, normal astrocytes will metabolize pyruvate using lactate dehydrogenase into lactate and 2 moles of ATP (anaerobic glycolysis). Neuronal neoplasms have been shown to do something much different: they preferentially metabolize pyruvate into lactate even when O_2 is present in excess. O_2 consumption is reduced, and although only 2 ATP per mole of glucose is produced by this process, significant stores of ATP are still present. This process was discovered by Otto Warburg and is now known as *aerobic glycolysis* or *the Warburg effect* (Warburg,

1956). This process is thought to confer upon the malignant astrocyte the ability to thrive whether oxygen is present or not, so long as there is a steady supply of glucose. As a consequence of this process, the metabolic activity of brain neoplasms must be assessed in terms of glucose uptake rather than O_2 consumption. Not surprisingly, positron emission tomography scans of astrocytomas show that cerebral glucose uptake and consumption by tumor may be up to 3 times that of normal brain.

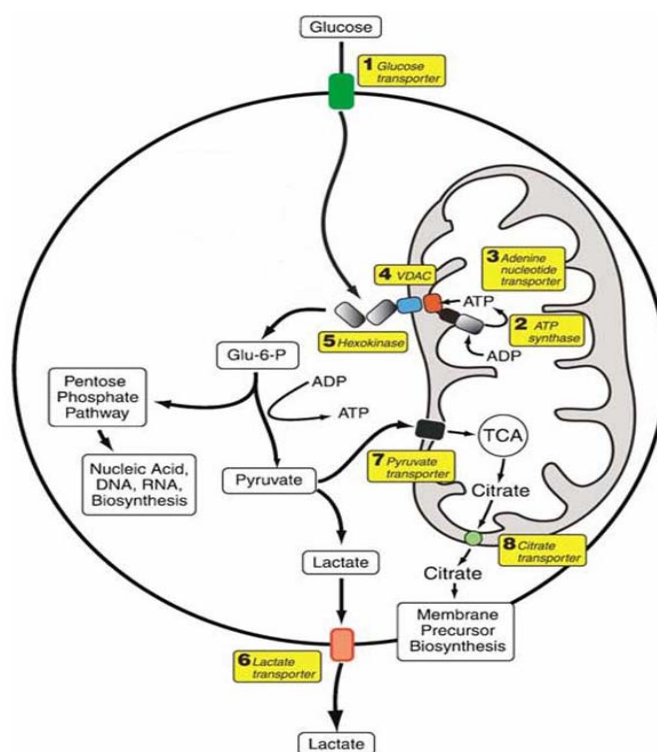


Figure 4: In tumor cells, hexokinase is found to be closely associated with the mitochondrial membrane. (Mathupala, Ko et al. 2006).

The Glycolytic Pathway - In 1956, after observing the high rates of glycolysis in many aggressive tumor cells and noting the absence of the Pasteur effect, Otto Warburg hypothesized that rapid anaerobic glycolysis was the primary explanation of malignancy (Warburg, 1956). This hypothesis has since been disproven by many observations, for example, many tumor cells utilize other substrates besides glucose (including lipids,

amino acids, and ketones). Furthermore, relative rates of glycolysis of some normal tissues overlap with the rates of glycolysis in tumor cells (such as rapidly dividing tissues in the gut, and in the embryo). Finally, mutant cell lines incapable of glycolysis have still retained their malignant characteristics (Dills, 1993). Nevertheless, rapid glycolysis is a frequent characteristic of malignant tumor cells. As we will discuss, there are several molecular reasons for the enhanced glycolysis in tumor cells.

Changes in Enzymes and Metabolic Patterns - Recall that the three rate-limiting enzymes of the glycolytic pathway are PFK-1, HK, and pyruvate kinase. A few researchers have published results showing a 30% to 60% decrease in PFK-1 activity and a 29% to 40% decrease in hexokinase activity in fresh GBM homogenates (Lowry et al., 1983; Marzatico et al., 1986). However, the vast majority of literature has shown a significant increase in the activity of each of the key regulatory enzymes in glycolysis in tumor cells (Argiles and Lopez-Soriano, 1990, 1998; Argiles and zcon-Bieto, 1988; Baggetto, 1992; Dills, 1993; Floridi et al., 1989; Gatenby and Gillies, 2004; Rodriguez-Enriquez and Moreno-Sanchez, 1998). These changes in enzyme activity appear to be unrelated to ATP or citrate levels, implying that in neoplasms, these enzymes are fundamentally different than they are in normal cells (either in cofactor requirements or in structure). Strong evidence supports the finding that the glycolytic rate is elevated in malignant tumors; modern day fdG PET studies have confirmed the massive increase in glucose metabolism in a great many brain tumors.

- **Hexokinase:** The K_m of hexokinase for glucose in tumor cells is even lower than that of wild-type HK (isoform II predominates in tumor cells, whereas type IV is seen in WT). HK exists in two forms in tumor cells: a cytosolic form and a

mitochondrial bound form. This is thought to confer a metabolic advantage to tumor cells, harnessing ATP generated from oxidative phosphorylation and shunting it directly into glycolysis (Figure 4).

- **Phosphofructokinase-1:** The rate-limiting enzyme of glycolysis in normal cells, PFK-1 activity is much increased in tumor cells. This is thought to be a result of a rise in lactic acid levels that increase the proton concentration in the cytosol (decreasing pH), which in turn stimulates PFK-1 (Rodriguez-Enriquez and Moreno-Sanchez, 1998). Furthermore, fructose 6-phosphate (a potent activator of PFK-1) is present in large amounts due to increased HK activity. This overcomes any inhibition that ATP may have on PFK-1, and the resulting fructose 1,6-bisphosphate activates not only PFK retroactively, but also PK proactively.
- **Pyruvate Kinase:** PK is a tetramer that may exist as different isozymes made up of either K or M subunits. The K or M2 type is dominant in fetal life, and is the only isoform found in malignant gliomas. M type is found in normal adult cells (Tolle et al., 1976) The M2 fetal type PK is strongly inhibited by alanine and activated strongly by fructose 1,6-bisphosphate. The result is rapid conversion of phosphoenolpyruvate to pyruvate by PK.
- **Lactate Dehydrogenase:** Lactate dehydrogenase activity is the same in tumor cells as it is in wild type cells, explaining the relatively high lactate levels found in and around tumors *in situ*. As we will soon discuss, the greatly reduced NAD⁺/NADH ratio in tumor cells greatly favors the rapid conversion of pyruvate to lactate.

It has been proposed that these isoenzymatic pattern changes are part of a metabolic strategy that tumor cells enact in order to survive in a low oxygen environment. There are currently three hypotheses that attempt to explain this observed phenomenon: A) gene mutation leads to isoenzymatic changes in key regulatory enzymes of glycolysis (PFK-1 and HK) which then lead to a change in the way these enzymes react to positive and negative stimuli; B) glycolysis is accelerated due to lack of activity in the transference systems of cytosolic reducing equivalents to mitochondria (malate/aspartate and glycerol-3-phosphate shuttles) resulting in conversion of much of the pyruvate from glycolysis into lactic acid, further decreasing cytosolic NADH oxidation, and C) the complex of pyruvate dehydrogenase is competitively inhibited by acetoin (a 4-carbon metabolite resulting from pyruvate non-oxidative decarboxylation) (Rodriguez-Enriquez and Moreno-Sanchez, 1998).

Enhanced Glucose Uptake - One of the contributing factors to enhanced glucose utilization in tumors is an increase in glucose uptake into the tumor cells. Most studies confirm that there is a significant increase in the numbers of the GLUT transporters in malignant cells. Furthermore, increases in glucose uptake into tumor cells may also be a result of the increased concentration gradient of glucose driving the molecule into cells (due to rapid glycolysis and lactic acid production inside of the cell) (Dills, 1993).

Lack of a Pasteur effect and Mitochondrial Content - Most tumor cells have a reduced or absent Pasteur effect, most likely due to lack of competition for ADP between glycolysis and respiration (as a result of the aforementioned changes in tumor glycolysis). Quite interestingly, it has been shown that the actual mitochondrial content of many of the fastest growing tumors is quite low (in concert with the observation of low

oxygen uptake by these same cells) (Dills, 1993).

The NADH Shuttles - Under normal circumstances, the NADH generated from the glycolytic pathway is normally shunted into the mitochondria for oxidation by several shuttles (malate/aspartate, glycerol-phosphate, or fatty acid cycle). In tumor cells, these shuttles are apparently impaired, and as a consequence NADH levels increase in the cytosol, leading to further lactate metabolism and NADH reduction in the cytosol. However, this appears to play a very minor role in excess lactate production since several researchers have shown that the shuttles (for example, the malate/aspartate shuttle) in several tumor cell lines is sufficient to fully re-oxidize cytosolic NADH (Greenhouse and Lehninger, 1976).

The ATP Synthase Activity of a Cell as Modulator of Glycolysis - Since ADP acts directly on the PK step of glycolysis as an up-regulator, it stands to reason that increased ATP synthase activity would serve to increase the rate of glycolysis by providing higher amounts of ADP to act at the PK step. Not surprisingly, ATP/ADP ratios have been shown to be significantly lower in several types of tumor cells. Furthermore, a defective Na/K ATPase has been discovered in tumor cells that acts with a high amount of inefficiency (increased ATP hydrolysis/Na extrusion ratio), apparently due to phosphorylation of the enzyme by a tyrosine kinase present in the membrane (Argiles and Lopez-Soriano, 1990).

The Citric Acid Cycle and Oxidative Phosphorylation - In malignant astrocytomas the activities of citrate synthetase and malate dehydrogenase are markedly decreased, while the activity of succinate dehydrogenase appears to be equal to that of normal cells. The result of this is that less acetyl-CoA is used by a less active TCA cycle.

Pyruvate will then accumulate (forming abnormally high levels of lactic acid) and NADH is not produced (so O_2 is not consumed by oxidative phosphorylation). Many researchers have concluded that the grade of malignancy of an astrocytoma is inversely related to its cytochrome oxidase activity (Allen, 1957, 1972). Other researchers have discovered a “truncated” TCA cycle in various malignant tumors. In these cells, citrate does not continue its oxidation because the aconitase and isocitrate dehydrogenase enzymes have low activity. Citrate is therefore actively released from the mitochondria where it is used for sterol/cholesterol synthesis in the cytosol (Rodriguez-Enriquez and Moreno-Sanchez, 1998) (Figure 5).

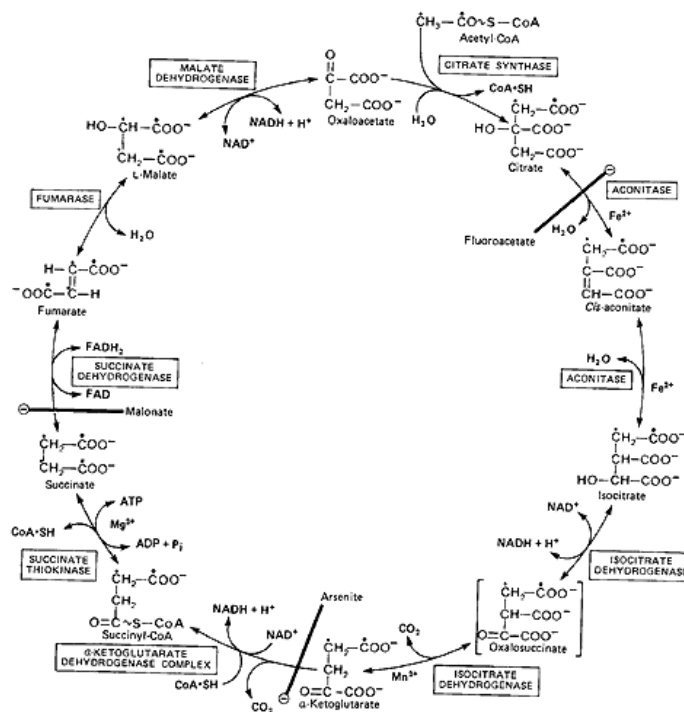


Figure 5: The citric acid cycle. In malignant tumors, the citric acid cycle is “truncated”, and citrate is shunted out of the mitochondria and used for sterol synthesis in the cytosol. (©Dr. Noel Sturm 2009 <http://chemistry.gravitywaves.com/CHE452/SyllabusCHE452SP09.htm>)

The Pentose Phosphate Pathway (Pentose Shunt or PPP) - The purpose of the pentose shunt is to metabolize glucose-6 phosphate (a glycolytic intermediate) via

glucose-6 phosphate dehydrogenase (the rate limiting enzyme of the PPP) to phosphoribosylpyrophosphate (PRPP) which is a precursor for purine and pyrimidine synthesis. Presumably because of the forward need for nucleic acid synthesis in rapidly dividing tumor cells combined with the fact that most of the metabolic pathways downstream of glycolysis are working so slowly, the activity of glucose-6 phosphate dehydrogenase has been found to be more than 280% that of normal brain.

Gluconeogenesis in the Host - Under normal circumstances, lactate metabolism in muscle is coupled to gluconeogenesis in the liver as lactate is shunted to the liver and converted to pyruvate and then to glucose. The presence of tumor in the host, much like an active muscle, causes increased Cori cycling in the host. However, in this case unless some sort of compensation occurs, this Cori cycling will reduce the amount of glucose available and/or increase the amount of energy required for gluconeogenesis. The end result of this process is cancer cachexia and death (Dills, 1993) The drug hydrazine sulfate is an inhibitor of gluconeogenesis from lactate and amino acids; it has shown some promise as a drug to treat cachexic cancer patients (Argiles and Lopez-Soriano, 1998) (Figure 6).

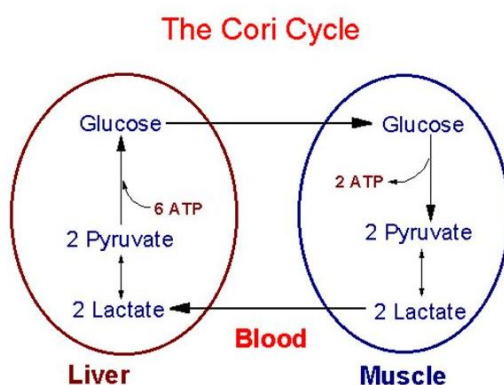


Figure 6: The Cori cycle. Tumor cells can be viewed as a replacement of or an addition to the active muscles in this figure. (web.indstate.edu/thcme/mwking/cori.gif)

The Tumor Metabolic Phenotype - As previously discussed, it has been well established that malignant tumor cells **aerobically** metabolize glucose into lactic acid (the Warburg effect) whether or not there is oxygen in adequate supply (loss of the Pasteur effect). Increased rates of glucose uptake in tumor cells have been shown through fdG PET studies, and the rate of glycolysis in cultured mammalian tumor cells has been positively correlated to tumor aggressiveness. Despite the fact that the Warburg effect appears (on the surface) to be detrimental to tumor cells, it is currently believed that this metabolic mutation confers a significant survival advantage to malignant cells (Gatenby and Gillies, 2004).

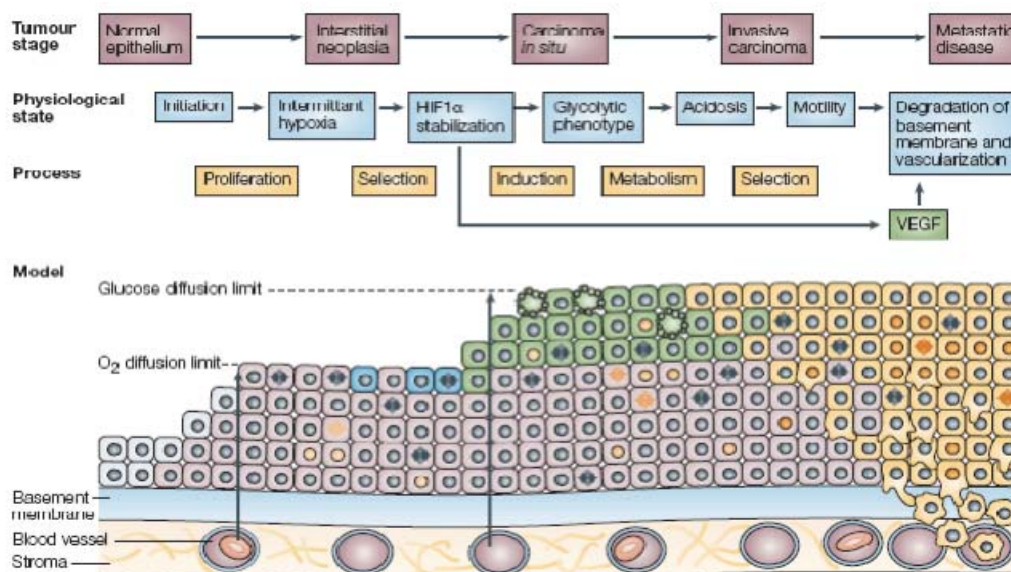


Figure 7: Tumor cells grow away from the basement membrane (i.e. away from their blood supply) and thus the ability for tumor cells to function metabolically whether oxygen is present or not confers upon those tumor cells a considerable evolutionary advantage over their host (Gatenby and Gillies 2004).

At first glance, the glycolytic phenotype appears to place the malignant tumor cell at a metabolic *disadvantage*. Only 2 net ATP are produced from the formation of lactate from pyruvate (whereas oxidative phosphorylation yields 38 net ATP). The metabolic

products of glycolysis result in a consistent acidification of the extracellular space, perhaps leading to cellular toxicity. So, why and how would these seemingly lethal disadvantages confer an evolutionary *advantage* to malignant cells? (Figure 7).

Pre-malignant lesions appear to be very well vascularized only in a macroscopic sense. When examined more closely, it is apparent that although a tumor may appear to have a very vascular stroma, the pre-malignant cell mass is separated from the blood vessels by a basement membrane. Oxygen tensions have been measured *in situ* in human malignant tumors. Cells adjacent to capillaries displayed a mean O₂ concentration of 2%, and cells located 200 micrometers from the nearest capillary displayed a mean O₂ concentration of 0.2% (Dang and Semenza, 1999). Assuming that this basement membrane stays intact, and understanding that there are finite limits to oxygen and glucose diffusion from the stromal capillaries through the basement membrane into the tumor, it is obvious that early carcinogenesis and development of the malignant phenotype actually occur in an *avascular* environment (Gatenby and Gillies, 2004). As proliferation continues pushing cells away from the basement membrane, pre-malignant lesions will develop an area of hypoxia at and outside of the oxygen diffusion limit. It is at this point where nature will favor cell phenotypes that are adapted to harsh environments with low substrate availability.

Normal cells respond to hypoxia by induction of the hypoxia inducible transcription factor HIF-1, a basic-helix-loop-helix (bHLH) factor that contains 2 subunits (HIF-1 alpha and HIF-1 beta). HIF-1 beta is also known as the arylhydrocarbon receptor nuclear translocator (ARNT). HIF-1 binds to the DNA sequence 5'-RCGTG-3' and increases the expression of glycolytic enzyme genes such as aldolase A, enolase

1, lactate dehydrogenase A, PFK, phosphoglycerate kinase, and pyruvate kinase M as well as the VEGF gene. Glycolytic enzyme gene regulation is also controlled at the carbohydrate response element (ChoRE; 5'-CACGTG-3'). The HLH-leucine zipper transcription factor USF2 binds at this site and also up-regulates the glycolytic genes (Dang and Semenza, 1999). It is also interesting to mention that apoptotic signals brought on by genotoxic exposure tend to have the opposite effect on glycolytic genes. That is, genotoxic exposure (DNA damage by cisplatin, etoposide, or gamma-irradiation) *down-regulates* key glycolytic enzyme genes (HK, PFK-1, and PK, among others) (Zhou et al., 2002).

Lactic Acid Metabolism in Astrocytomas - So far, we have established that malignant tumor cells preferentially undergo “aerobic glycolysis”, i.e. when presented with glucose as a substrate tumor cells rapidly metabolize it into lactate regardless of the state of oxygenation of the cell. We have also discussed the loss of the Pasteur effect (inhibition of glycolysis in the face of adequate oxygen content) and gain of the Crabtree effect in tumor cell glycolysis (glycolysis proceeds independent of oxygen content and cannot be regulated). As described, this metabolic pathway is certainly a large part of the unique tumor metabolic phenotype (although not the only part) and therefore has served as a therapeutic target for many cancer researchers. However, there has been new research into the nuances of lactate metabolism that may serve to reverse many of the preconceived notions of lactate’s role in the cell.

For many years lactate has been considered a useless end product of anaerobic energy metabolism, and if allowed to accumulate, could become harmful. Recent research, however, has shown that lactate actually plays a transient, yet major role in

aerobic energy metabolism in the normal brain (Schurr, 2006). Central to this notion is a hypothesis by Magistretti and colleagues known as the astrocyte-neuron lactate shuttle hypothesis (ANLSH). Normal astrocytes were found to respond to neuronal activity mediated by the neurotransmitter glutamate by increasing glucose consumption and producing more lactate. In parallel, neurons preferentially oxidize lactate present in the extracellular space rather than glucose to meet their energy demands (Pellerin and Magistretti, 2004). Supporting this hypothesis is a functional imaging study using two photon spectroscopy demonstrating spatiotemporal partitioning of glycolytic and oxidative metabolism between astrocytes and neurons during focal neuronal activity, establishing a unifying hypothesis for neurometabolic coupling between early oxidative metabolism in neurons and late activation of the ANLS (Kasischke et al., 2004) (Figure 8).

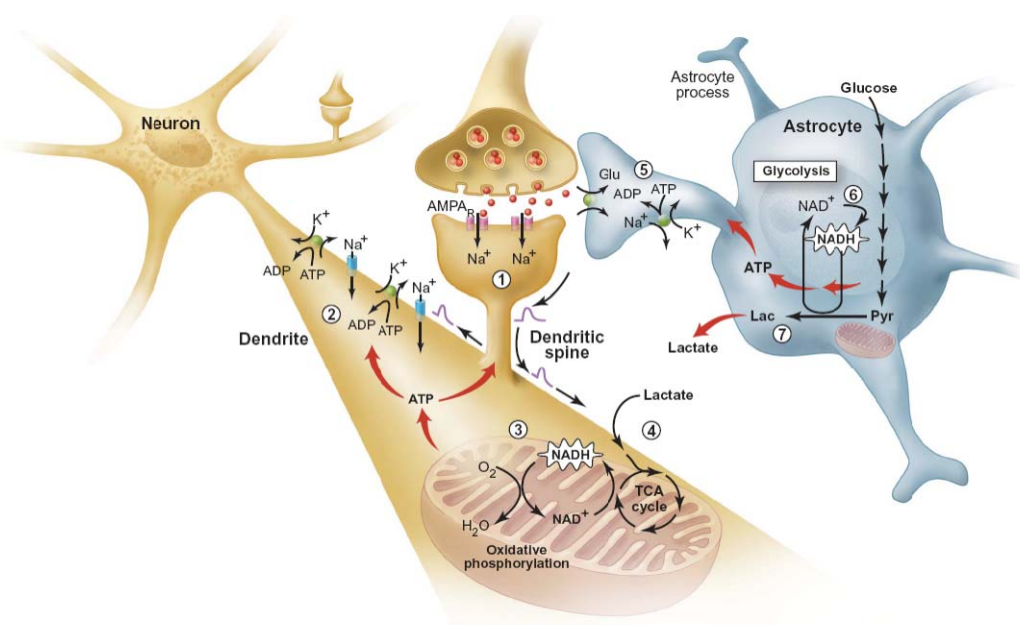


Figure 8: The astrocyte-neuron lactate shuttle hypothesis (ANLSH). Normal astrocytes, in a supporting role for surrounding neurons, will take in glucose and metabolize it to lactate, which is then shunted out of the astrocytes and taken up by the surrounding neurons. This lactate then enters the TCA cycle of neurons in their mitochondria where NADH is oxidized to generate ATP (Pellerin and Magistretti 2004).

Many studies have shown that glutamate uptake stimulates astrocytes to produce and secrete lactate to feed neurons *in vitro* and *in vivo*. Kasischke and colleagues used two-photon fluorescent spectroscopy and confocal microscopy to examine NADH concentration (a signature of glycolysis or oxidative phosphorylation) in the CA1 region of the rat hippocampus through stimulation of the Schaffer collateral pathway. At low magnification of the confocal microscope the tissue presented a biphasic response: an initial “dip” in the NADH level followed by an “overshoot”. Upon closer confocal magnification it was observed that the “dip” in the fluorescent signal and return to baseline was restricted to the dendrites of neurons in a small area of the hippocampus. Since this signal originated from the mitochondria, this data was interpreted as a burst in oxidative phosphorylation (and NADH consumption) followed by activation of the TCA cycle to regenerate NADH. The late “overshoot” fluorescent signal was located in the cytoplasm of the processes of astrocytes. This signal was interpreted as a burst in glycolysis in which large amounts of cytoplasmic NADH is generated before being converted back to NAD⁺ as lactate is produced (Kasischke et al., 2004; Pellerin and Magistretti, 2004). These metabolic processes are separated temporally, spatially, and pharmacologically (the oxidative response in neuronal dendrites could be inhibited by AMPA/kainate receptor activation whereas the glycolytic response in astrocytes could not, indicating that the former was a postsynaptic response and the latter was presynaptically triggered). These findings strongly support the theory of the ANLSH and some researchers have gone so far as to hypothesize that it is *lactate* and not pyruvate that is the end product of cerebral glycolysis and that lactate is the central fuel that feeds into the citric acid cycle (Schurr, 2006). Other 13C

and ^1H studies demonstrated two metabolic pools of lactate and pyruvate, and that exogenous lactate was the major substrate for oxidative metabolism of glioma cells and the other pool was related to aerobic glycolysis (Bouzier et al., 1998). Whether or not these hypotheses are indeed correct, there is undeniable evidence that shows production of significant amounts of lactate in tumor cells. Glioma cells have a very efficient method of removing excess lactate (not used in metabolism) from the cytoplasm in order to keep intracellular pH at a working level.

Monocarboxylate Transport

Lactate was once thought to be removed from cells via simple diffusion through the membrane. Recent studies, however, have identified a family of monocarboxylate transporters (MCTs) that facilitate the passive transport of lactate across the plasma membrane. These transporters work as symporters, effluxing lactate with H^+ for example. There are at least 14 members of the MCT family found in the human genome (the so-called SLC16 gene family), however only 4 of these (MCT 1-4) appear to be functional (Halestrap and Price, 1999). These MCTs transport lactate and H^+ out of the cytosol, thus leading to an increase in intracellular pH. However, these are not the only means by which tumor cells may regulate pH (Mathupala et al., 2007). Transmembrane studies have shown that tumors may use gradients such as sodium to exchange H^+ via the sodium-hydrogen ion exchanger (Gillies et al., 1990) or the Na^+ dependent $\text{Cl}^-/\text{HCO}_3^-$ exchanger (Lee and Tannock, 1998). These cells were shown to be at or even above normal physiologic pH. This has been confirmed in ^{31}P Magnetic Resonance Spectroscopy (MRS) studies of *in situ* tumor cells (Stubbs et al., 1999).

In order for MCTs to serve as viable targets for clinical therapeutics in malignant

tumors, they must differ significantly from wild type MCTs in level of expression, isotype expression, or both. MCTs 1 and 2 are highly expressed in malignant glioma (Mathupala et al., 2004) whereas MCT 3 (formerly known as type 4) predominates in normal brain. The function of MCTs can be disrupted by 1) small molecule inhibitors such as cinnamic acid derivatives, 2) by targeting their expression with post transcriptional gene-silencing strategies, or 3) by targeting accessory membrane proteins like gp70 and CD147 (Mathupala et al., 2007). In human cultured glioblastoma cells, the small molecule MCT inhibitor alpha-cyano-4-hydroxy-cinammic acid (ACCA) was successful in increasing intracellular lactate in tumor cells, shrinking tumor bulk, and upon exposure to low dose radiation caused rapid morphological changes in the tumor cells that led to apoptotic cell death (Colen et al., 2006). Through post-transcriptional gene silencing techniques, MCT 1 and 2 down regulation led to a decrease in efflux of lactate in tumor cells by 85% and significant necrosis in the tumor, however it only led to a pH reduction by 0.6 units (Mathupala et al., 2004). This result is likely explained by the aforementioned additional regulators of intracellular pH. Similar findings were obtained using the MCT inhibitor quercetin in rat C6 glioma cells (Volk et al., 1997).

Preliminary Data

MCT2 Proximal Promoter Harbors cis-elements that Respond to Glycolytic Metabolism and Erythropoietic Signaling - As part of ongoing research in the Principal Investigator's laboratory, a gene-library clone search on human genome data linked to clone archives of the Human Genome Project via the National Center for Biotechnology Information (NCBI) server in 2004, to locate a clone harboring the

monocarboxylate transporter-2 (MCT2) gene. A Fosmid clone (pFOS) was located which straddled the chromosomal location (chromosome location 12q14.1) for MCT2 gene. The clone was obtained and Fosmid DNA isolated, digested with restriction enzymes. Based on *in silico* mappings of the chromosomal region, a BamH I fragment that harbored a 4.2 kbp region of the MCT2 proximal promoter and the first exon was identified, gel-purified and cloned into plasmid pUC18. This was sequenced to verify identity of the sequence with information from *in silico* analysis.

Once the BamH I clone was confirmed to contain the MCT2 promoter by sequencing, the 4.2 kbp MCT2 promoter was cloned into pGL2-luciferase reporter gene vector (Promega) (Figure 9).

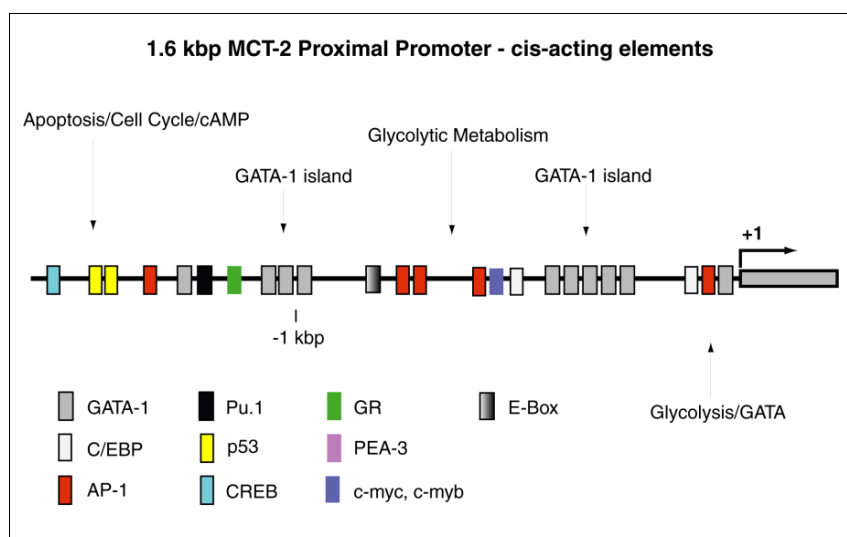


Figure 9: The upstream promoter for the monocarboxylate transporter 2 (MCT-2) gene. Several sequences upstream from the MCT-2 gene were found to be homologous to binding domains for many well-known regulatory proteins such as GATA-1, p53, c-myc, c-myb (all tumor suppressor proteins), AP-1 (part of the protein kinase C pathway), and CREB (Figure from Mathupala, NIH grant). Sequence map is displayed for the proximal 1.6 kbp region of the MCT-2 promoter within the 4.2 kbp Bam H1 clone. Individual response elements identified by sequence analysis are indicated within the figure.

Primary GBM Tissue and U-87MG Glioma Cells Express GATA-1 at High Levels -

Based on our identification that multiple GATA-1 elements are present on the proximal

MCT2 promoter, a search of the currently available scientific literature was carried out, which indicated that expression of GATA-1 had not been reported, nor examined to date, either in experimental brain tumor cell lines or in primary brain tissues (normal or pathological). Thus, we undertook the following studies in 1] U-87MG glioma cells, 2] in normal brain tissue, and 3] in primary GBM tissue. Normal human brain tissues were obtained from autopsy specimens. GBM tissue specimens that contained >90% tumor (from surgical specimens accrued through institutional approved clinical protocols; Dr. Andrew E. Sloan) were used in the study.

Analysis of U-87MG Glioma Cell Line for Expression of GATA-1 - U-87MG cells growing under exponential culture conditions were washed in cold PBS and lysed *in situ* using a lysis buffer consisting of 50 mM sodium phosphate, pH 7.5, 10 mM Glucose, 10 mM 1-thioglycerol, 0.1% Triton X-100, 1% NP-40, supplemented with a protease inhibitor mix (Roche Molecular Biochemicals, Indianapolis, IN). Protein concentrations of diluted homogenates were assayed by the Bradford method and 5 to 20 μ g of total protein were resolved by SDS-PAGE (10%) (Figure 10). Thus, U-87MG glioma cells (which show a high glycolytic phenotype) express GATA-1 (~ 47 kDa), and is a suitable experimental model for both *in vitro* and *in vivo* studies described below.

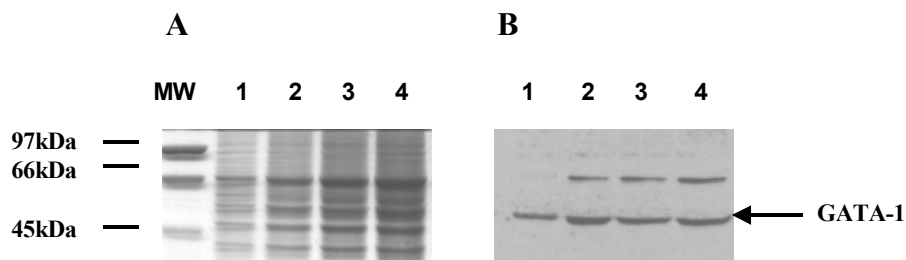


Figure 10: Lane 1, 5 mg; lane 2, 10 mg; Lane 3, 15 mg; Lane 4, 20 mg total protein respectively. Panel A: SDS-PAGE profile; Panel B: Western blot using GATA-1 polyclonal antibody (Novus Biologicals).

Analysis of Normal and GBM Brain Tissue for Expression of GATA-1 - As described above two normal brain tissue specimens and three GBM tissues were examined by western analysis for the presence, and expression levels of GATA-1. In brief, frozen tissue were sectioned into 0.5 mm slices, washed x3 in ice-cold PBS to remove residual blood (presence of which may give false-positive readings) and homogenized in the lysis buffer described above. 25 μ g aliquots of total protein were resolved by SDS-PAGE (10%) and expression of GATA-1 analyzed by western blotting (Figure 11).

Thus, GBM tissue express GATA-1 at much higher levels in comparison to that for normal brain tissues, which minimally express the transcription factor.

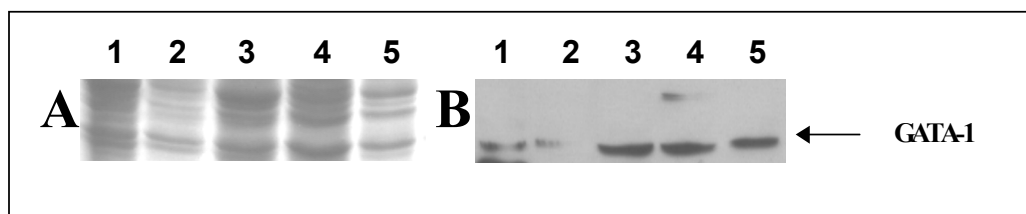


Figure 11: Panel A, SDS-PAGE; Panel B, Western blot for GATA-1. Lane 1, normal brain-surgical resection during decompression procedure, 25 μ g total protein; Lane 2, autopsy specimen (45 min post-mortem), 25 μ g total protein; Lanes 3-5, GBM tissue with >90% tissue incidence of tumor, 25 μ g total protein per lane

The data presented above provides GATA-1 protein expression patterns in normal and malignant brain tissues, as well as in one established experimental brain tumor cell-line we plan to use during our investigations. Normal or malignant brain tissues have not been examined for their GATA-1 status in literature to date. Thus, the data presented above is novel, and, with our previous evidence for the presence of GATA-1 cis-elements on the MCT2 promoter, provides additional proof that a GATA-1 mediated signaling system may be present in malignant brain tumors to maintain a

highly glycolytic phenotype.

Our current interest in GATA-1 stems from the fact that GATA islands have been identified in the upstream promoter segment of the gene for MCT-2 (recall that MCT isoform 2 is highly expressed in glioblastoma cells). It has been implied that downregulation of GATA-1 protein will result in decreased transcription of MCTs, thus leading to lactate buildup inside of the tumor cells and tumor death (in spite of other mechanisms for proton removal from the cytosol such as sodium-hydrogen exchangers). The above data is part of my advisor's NIH RO1 grant and is central to my specific aims. Surprisingly, central to this new therapy is a protein that, in the normal state, regulates the production of millions of perfectly normal red blood cells.

GATA Family of Transcription Factors

GATA-1 and Erythropoietin - The maturation of immature red blood cell precursors (proerythroblasts) into mature erythrocytes is normally under the control of a polypeptide hormone called erythropoietin (EPO), which promotes proliferation and survival of erythroid precursors (Orkin and Weiss, 1999). When an erythropoietin molecule binds the erythropoietin cell surface receptor on erythroblasts, it induces and/or stabilizes an anti-apoptotic protein called bcl-x. When researchers studied down-regulation of red blood cells more closely (through the use of caspases and cell surface death receptors on proerythroblasts on culture), researchers found that either deprivation of erythropoietin or activation of cell surface death receptors (i.e. Fas and Fas ligand, FasL) on erythroid cells leads to caspase-induced cleavage of a nuclear transcription factor called GATA-1. This molecule has been found to be crucial for erythroblast maturation and survival (Orkin and Weiss, 1999). GATA-1 is abundant in

erythroid precursors, and also has been found to strongly induce expression of bcl-x (cooperating with EPO).

The GATA family consists of 6 transcription factors (GATA-1 through GATA-6). All of these proteins bind the DNA consensus sequence (A/T)GATA(A/G) via 2 characteristic C₄ zinc finger motifs (Cys-X₂-Cys-X₁₇-Cys-X₂-Cys) (Ferreira et al., 2005). GATA-1 was first identified as a protein with binding specificity to Beta-globin 3' enhancer and the gene for GATA-1 is localized to Xp21-11. GATA-1 is essential for normal erythropoiesis and GATA-1 deficient mice are unable to produce mature erythrocytes. GATA-1 also plays a role in megakaryocyte regulation and eosinophil development. It has been implied that GATA-1 is directly involved in cell survival through its activation of EpoR erythropoietin receptor and its known target gene Bcl-XL (an anti-apoptotic protein). A variety of GATA-1 target genes have also been hypothesized to be involved in cell cycle regulation and/or proliferation and differentiation processes.(Ferreira et al., 2005).

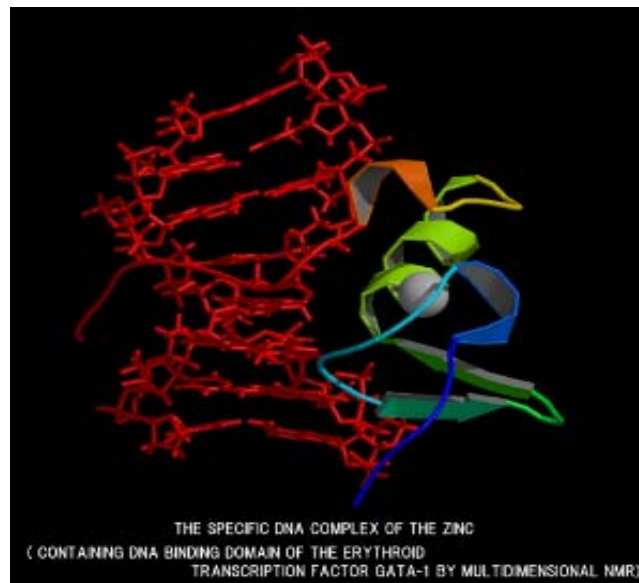


Figure 12: The DNA binding domain of the GATA-1 molecule contains a novel structure that resembles cys-cys variety zinc finger domains. (gibk26.bse.kyutech.ac.jp/jouhou/image/dna-protein/all/small_N1gat.png)

Short DNA sequences within control elements of genes constitute *cis*-regulatory motifs recognized by nuclear proteins that participate in transcription. Through studies of hematopoietic stem cells, GATA-1 became a well known *cis*-acting regulatory element in several other gene promoters besides those that control hematopoiesis, for example platelet factor 4, mast cell carboxypeptidase A (MC-CPA), preproendothelin-1, and vascular cell adhesion molecule-1 (VCAM-1) (Orkin, 1992). GATA motifs upstream of genes have various roles, but predominately these sequences (when bound to GATA-1) act as upstream promoters, enhancers, and locus control regions (LCRs). The individual GATA sequences may vary, and may be present in varying degrees of complexity.

Members of the GATA-binding protein family are related by a highly conserved protein domain necessary and sufficient for DNA-recognition. The DNA-binding domain is characterized by a novel structure: 2 homologous finger domains that resemble cysteine zinc fingers (Orkin, 1992; Tang et al., 2001) (Figure 12). These domains are very highly conserved among mammals, avians, and amphibians. There so far have been roughly 8 different GATA binding proteins (defined as GATA-1 through GATA-8), but the most well known are GATA-1 through GATA-4. GATA-1 has also been called “the erythroid transcription factor”, as it is hematopoietic specific and abundant in erythroid, megakaryocytic, and mast cell lineages (Orkin, 1992). Because GATA-1 has been also identified in pluripotent mouse and human cell lines, it is thought to be expressed in multipotential progenitor cells and expression maintained thereafter. GATA-2 and GATA-3 are found in megakaryocytes, T-cells, and mast cells, while GATA-4 enjoys very little tissue expression.

Project Outline and Hypothesis

There are many unique features of tumor cells (Glioblastoma, in particular) that represent potential targets for gene therapy. The main thrust of my research proposal is to target one of these unique features, namely the monocarboxylate transporter, using a novel method of translational regulation. Glioblastoma cells purposefully modify their own biochemistry to undergo “aerobic glycolysis” and lactic acid fermentation even in the presence of ample oxygen. The excess lactic acid produced by the tumor cells is rapidly shunted out of the tumor cell cytosol by the aforementioned cell membrane transporters, creating a toxic acidic microenvironment favoring tumor invasion as well as an acceptable intracellular pH allowing basic enzymatic function to continue. Down-regulation of this transporter (using a variety of methods including the drug *α*-cyano-4-hydroxycinnamic acid) has been shown to arrest and even retard the growth of Glioblastoma cells *in vivo* and *in vitro*. It is my goal to block the transcription of lactate transporter isoform 2, which has been shown to be up-regulated in Glioblastoma cells. I will accomplish this by using small interfering RNA (siRNA) against mRNA transcripts of GATA-1 protein, a recognized transcription factor for the promoter of lactate transporter isoform 2. I will first demonstrate that siRNA against GATA-1 delivered to U87-MG Glioblastoma tumor cells *in vitro* via liposome transfection results in decreased GATA-1 protein. I will also simultaneously determine the anti-GATA-1 siRNA sequence most effective at producing this decrease. Next I will use a retroviral vector to examine the efficiency of anti-GATA-1 siRNA induced GATA-1 transcription inhibition on cell growth, apoptosis, and metabolism (in particular, lactate metabolism) *in vitro*.

The second phase of this project will attempt to test the opposite situation from

phase 1; that is, we will use a different set of plasmids to over-express GATA-1 in U-87MG tumor cells and examine the effects this will have on proliferation of the tumor cells, the cell cycle, MCT-2 expression and gene transcription, and lactate efflux and metabolism.

Experimental Methodology

Small Interfering Ribonucleic Acids [siRNAs] and Gene Downregulation: Gene Transcription and Translation and Gene Silencing - Deoxyribonucleic Acid (DNA) is composed of a double helix of two long chains of covalently linked deoxyribonucleotides (adenine, guanine, cytosine, and thymidine). The two DNA strands have 5' and 3' ends and normally are bound to each other (A to T and C to G). The strands contain identical information (in normal circumstances, i.e. excluding mutations or translocations) but are linked together in opposite directions such that the sense strand is read from 3' to 5' and the antisense (or template strand) is bound to it from 5' to 3'. Gene transcription (the formation of messenger RNA from native DNA) takes place in the nucleus of the cell. Certain transcriptional enzymes unfold the chromosomal DNA and others (like RNA polymerase) separate the helix and read the template strand (only) from 5' to 3' and synthesize long single strands of messenger ribonucleic acid (mRNA). Gene translation takes place in the rough endoplasmic reticulum (rER) of the cytoplasm. Ribosomes (made up of ribosomal RNA or rRNA) recognize distinct 3-base pair long codons in the mRNA and match these up to complementary 3-base pair sequences on transfer RNA (tRNA) molecules that are linked to amino acids. The Genetic Code determines which specific amino acids are linked to which specific codon (there is overlap and there also are specific start codons that signal the ribosome to begin translation and stop codons

that signal the ribosome to fall off of the mRNA strand).

It stands to reason that if a researcher knows the specific sequence of base pairs of a gene or genes of interest, then he/she would be able to synthesize *antisense RNA* against that sequence (that is, a single strand of RNA that is complementary to the single strand mRNA copy of that gene). When introduced into the cytosol, theoretically these sequences would (by Brownian motion) seek out their complementary mRNA sequence and bind to it, forming a double strand of mRNA and rendering it unreadable by the ribosomes (which can only translate single stranded mRNA into proteins). In general, this method is very ineffective at down-regulating proteins, and a more specific method is needed to apply this principle *in vivo*.

In their work on nematodes and the protein *unc-22* (important for muscle function), Andrew Fire and Craig Mello (eventual Nobel prize winners in medicine) had witnessed the failure of single stranded antisense RNA against this protein, and had witnessed that it had appeared that sense RNA seemed to work similarly to antisense RNA. They (correctly) predicted that it was actually *double stranded RNA* that was the culprit for the apparent initial success of antisense RNA. They guessed (again, correctly) that previous preparations of “single stranded” antisense RNA was contaminated with a small amount of “sense” RNA which then annealed to its complement antisense RNA before re-introduction into the cytosol. Sure enough, when double stranded sense and antisense RNA against the *unc-22* gene was introduced into nematodes, uncontrollable twitching of the nematode ensued (evidence of muscle protein dystrophy by knockdown of *unc-22*). The field of “RNA interference” was born (Lau and Bartel, 2003) (Figure 13). The essence of this newly discovered host cell

machinery is as follows: small foreign pieces of double stranded RNA in the cytosol are recognized by the protein “DICER” and cleaved into small fragments (termed “small interfering RNAs”). Single strands of these fragments then are loaded onto “RISC” proteins which then seek out RNA sequences that are homologous to the sequences to which they are attached. If a RISC complex binds a homologous RNA sequence, it activates a host of cell machinery (including DICER and exonucleases) and degrades that RNA strand.

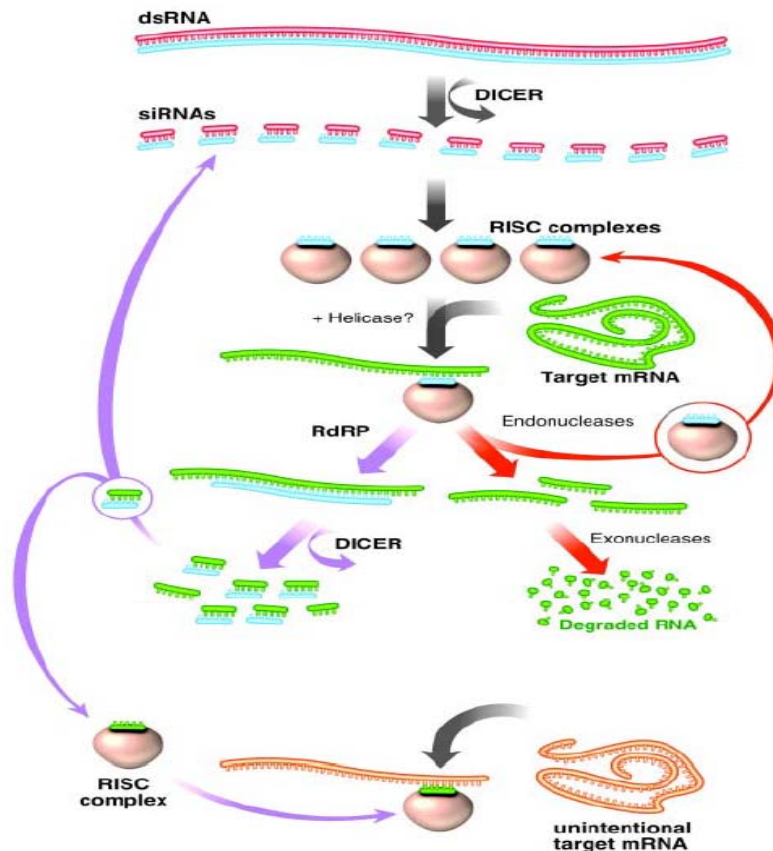


Figure 13: Double stranded RNA is recognized by the cytosolic protein DICER as foreign and is cleaved into small interfering RNAs (siRNAs). These siRNAs bind RNA-induced silencing complexes (RISC) molecules to form activated RISC complexes (RISC*). RISC is thought to have helicase and endonuclease activity (or may be associated with other enzymes). If a RISC complex encounters an mRNA sequence that is complementary to the sequence that it carries then that mRNA molecule is cleaved and degraded. This may be foreign mRNA (i.e. viral) or even native mRNA molecules.

Application of RNA Interference to Brain Tumor Research - RNAi induced by synthetic hairpin RNAs (shRNAs) has recently been used to study gene function in plants and animals and has been shown to silence genes in much the same way as siRNAs (Matzke and Matzke, 2003). siRNAs are roughly 25 nucleotides long, and are complementary to both the sense and antisense strands of mRNA (suggesting a double stranded origin). Evolutionarily, they may have had a role in silencing transposable elements, repetitive genes, or viruses (Novina and Sharp, 2004; Sharp, 1999).

Once siRNA is in the cytosol, it binds to RNA-induced silencing complexes (RISC) to form activated RISC (RISC*). RISC* now is capable of binding an mRNA strand (single stranded) complementary to the siRNA that it carries in the cytosol and bringing about its degradation. There is evidence that the 5' end of the siRNA is the ruler for position of subsequent cleavage, and a 5' phosphate is required on the target mRNA (Martinez et al., 2002). In fact, the 5' end of the siRNA fragment bound to RISC has been shown to be necessary and essential to RNAi activity (Chiu and Rana, 2002).

This presents an exciting new application to brain tumor research. SiRNA is nonselective, that is, it can trigger degradation of native mRNA transcripts as well as foreign ones. Therefore, purposeful injection or introduction of siRNA molecules against a known mRNA sequence could very selectively knock down that protein in the cell (Ezzell, 2002). There are essentially three potential sites for therapeutic intervention: transcriptional, post-transcriptional, and post-translational. Most drugs target post-translational molecules. SiRNA has the ability to target peptides before they are even peptides i.e. target the mRNA that codes for them (Shuey et al., 2002). A very clear target in the malignant tumor cell is the aforementioned lactate transporter. Essential to

tumor cell survival and isoforms that are unique to glioblastoma, the lactate transporter offers an attractive target for post-transcriptional therapy.

The selection and design of siRNA molecules is challenging. The keys to siRNA-dependent gene silencing depend upon a number of critical factors: target sequence selection and siRNA design, suitable cell line or culture system, optimized delivery conditions, abundance and turnover rate of the target mRNA or protein of interest, and accuracy and ease of assaying for mRNA levels, protein levels, or phenotype. We chose the Dharmacon SMARTpool siRNAs (Dharmacon, Inc.) which incorporate several features optimum for effective silencing: 21-nucleotide RNA oligonucleotides forming a 19-base pair duplex core, symmetrical 2 nucleotide 3'-UU overhangs, 5'-phosphorylated antisense strand, desalted and quality controlled (average molecular weight = 13,300 g/mole, confirmation of duplex formation by non-denaturing gel electrophoresis) (Figure 14).

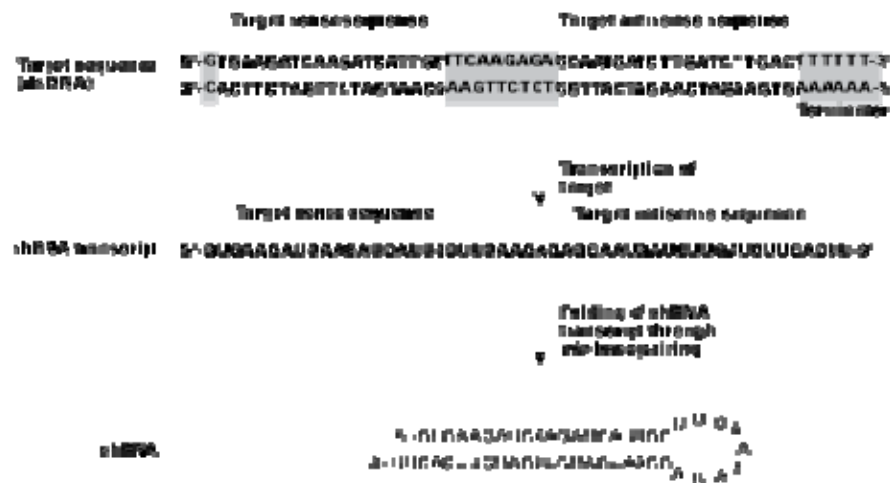


Figure 14: Example of a small hairpin RNAs (shRNAs) generated from an oligonucleotide DNA sequence from the beta-actin gene. A hairpin loop is located between the sense and antisense sequences on each complementary strand. The shRNA acts like siRNA molecules capable of carrying out gene-specific silencing. (from “Knockout Inducible RNAi Systems User Manual,” Clontech Laboratories, Inc., Mountain View, CA)

Inducible RNAi expression systems; (Tet-On, Tet-Off systems) - One of the most efficient methods of down-regulating a given protein's production in laboratory cultured cells is to transform those cells using an inducible vector with the gene of interest. We chose the tetracycline transactivator system (Clontech). This system can be programmed to either turn production of our gene of interest (in our case, siRNA genes) on or off in the presence of tetracycline or doxycycline. We chose the tet-on system and it works as follows: our gene of interest is spliced into a vector downstream (and controlled by) an inducible promoter. This promoter is off at baseline as the activator cannot bind to the promoter without doxycycline. As doxycycline is added to cell media, it binds the activator which then is allowed to bind the promoter and our gene of interest is synthesized (Figure 15).

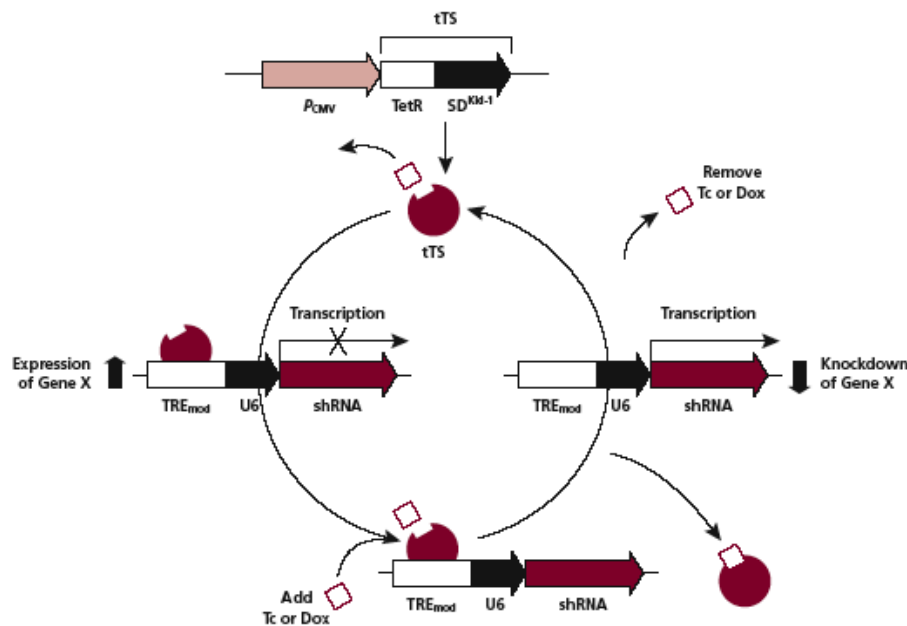


Figure 15: Schematic of gene regulation in the inducible tTS system. The suppressor tTS binds the *tetO* sequence in the TRE(mod) promoter region of the response plasmid, suppressing shRNA expression. In the presence of doxycycline or minocycline, the tTS dissociates from the TRE(mod) and allows activation of shRNA transcription from the downstream U6 promoter. [From the “Knockout Inducible RNAi Systems User Manual”, Clontech Laboratories, Inc.]

CHAPTER 2

EFFECT OF DOWN-REGULATION OF GATA-1 AND EXPRESSION IN GLIOMA CELL LINE U87-MG

Introduction

From our prior work we know that there are GATA-1 regulatory islands in the proximal MCT-2 promoter (preliminary data from NIH grant5R01 CA116257 (NCI/NIH) Mathupala, S.P. Ph.D. (PI) Lactate Transport as a Therapeutic Target in Glioma). From the same preliminary data, we also know that GATA-1 protein is overexpressed in GBMs (both in GBM cell lines and in human primary GBMs from surgical specimens). The logical question that presents itself from these data is the following: What role does GATA-1 play in tumor metabolism? More precisely, what role does GATA-1 play in the regulation of MCT-2 protein in U87-MG tumor cells?

In order to examine the role of GATA-1 more thoroughly, we used a relatively new technique taking advantage of host cell machinery to knock down GATA-1 nearly completely in tumor cells. We began by using simple liposomes to deliver 4 distinct siRNA sets against GATA-1 to cultured U87-MG cells and measured the ensuing knockdown of GATA-1 via western blot analysis. We then designed short hairpin RNA molecules (shRNA) based on the siRNA data. We then engineered a Moloney Murine Leukemia Virions (MOMLV) to deliver shRNA-containing plasmids at high efficiency to cultured U87-MG cells, creating stable transformed cell lines that can produce shRNA against GATA-1 on our command via administration of doxycycline or minocycline. Through western blots we then looked at the effect of down regulation of GATA-1 on levels of MCT-2 protein in transformed U87-MG.

Design of siRNA, Theory, and Transfection Methods: The mRNA Sequencing of GATA-1 and Location of siRNA Targets

In order to fully utilize the technology of siRNA mediated gene silencing, a few pieces of data are needed. We need to know the sequence of the gene that we intend to target. We then need to select several different sequences within that gene that are relatively unique sequences (i.e. sequences that are unique to the gene of interest to avoid cross reaction of our siRNA with other mRNA transcripts). We also need a non-conserved sequence of mRNA that is not found in any known gene in the human genome (in this project we will be using human glioblastoma cells). This will serve as a control sequence. Once we have selected these unique sequences we can then passively transfect these sequences into our cells of interest and test which sequence is most effective at knocking down the level of protein that we are targeting. In our case, that protein is GATA-1.

The first step in the process involves a search on the NCBI website for the sequence of the GATA-1 protein. This site can analyze the sequence for the consensus sequence for the given protein (i.e., there may be several different DNA sequences leading to GATA-1, this site helps us find the sequences that all of the variations have in common). The end result of this is a cDNA sequence representing the GATA-1 gene.

cDNA for human GATA-1

```

1   gcaaaggcca aggccagcca ggacaccccc tgggatcaca ctgagcttgc cacatcccca
61  aggcggccga accctccgca accaccagcc caggtaatc cccagaggct ccatggagtt
121 ccttggcctg gggtccttgg ggacctcaga gcccctccc cagtttggg atcctgctct
181 ggtgcctcc acaccagaat caggggtttt ctcccctct gggcctgagg gcttggatgc
241 agcagcttcc tccactgcc cgagcacagc caccgctgca gctgcggcac tggcctacta
    [siRNA#1 308-324]
301 cagggacgct gaggcctaca gacactcccc agtctttcag gtgtacccat tgctcaactg
361 tatggagggg atcccagggg gctcaccata tgccggctgg gcctacggca agacggggct
421 ctaccctgcc tcaactgtgt gtcccaccg cgaggactct cctcccagg ccgtggaaga
481 tctggatgga aaaggcagca ccagcttctt ggagactttg aagacagagc ggctgagccc
541 agacctcctg accctgggac ctgactgcc ttcactctc cctgtcccca atagtgtta
601 tgggggccct gactttcca gtaccttct ttctcccacc gggagcccc tcaattcagc

```

661 agcctattcc tctccaagc ttcgtggaac tctccccctg cctccctgtg aggccagggg
 [siRNA #3 768-786]
 721 gtgtgtgaac tgcggagcaa cagccactcc actgtggcgg agggacagga caggccacta
 781 cctatgcaac gcctgcggcc tctatcacia gatgaatggg cagaacaggc ccctcatcc
 [siRNA#2 843-861]
 841 gcccaagaag cgccctgattg tcagtaaacg ggcaggtact cagtgcacca actgccagac
 901 gaccaccacg aactgtggc ggagaaatgc cagtggggat cccgtgtgca atgcctgcgg
 961 cctctactac aagctacacc aggtgaaccg gccactgacc atgcggaagg atggtattca
 1021 gactcgaaac cgcaaggcat ctggaaaagg gaaaaagaaa cggggctcca gtctgggagg
 [siRNA#4 1103-1122]
 1081 cacaggagca gccgaaggac cagctgggtg ctttatggtg gtggctgggg gcagcggtag
 1141 cgggaattgt ggggaggtgg cttcaggcct gacactgggc cccccaggta ctgccatct
 1201 ctaccaaggc ctgggacctg tgggtctgtc agggcctgtt agccacctca tgccttccc
 1261 tggacccta ctgggtcac ccacgggctc cttcccaca ggccccatgc cccccaccac
 1321 cagcactact gtggtggctc cgctcagctc atgagggcac agagcatggc ctccagagga
 1381 ggggtggtgt cttctcctc tttagccag aattctggac aaccaagtc tctgggccc
 1441 aggcacccc tggcttgaac cttcaaagct tttgtaaat aaaaccacca aagtcctgaa
 1501 aaaaaaaaaa aaaaaaaaaa aa

We then obtained 4 distinct pre-selected candidate siRNAs against GATA-1 (Dharmacon RNA Technologies, siGENOME ON-TARGETplus set of 4 duplex LQ-009610-00-0002 Human GATA1), these were arbitrarily defined as #1, #2, #3, and #4. These sequences are noted in red in the above sequence of the GATA-1 gene.

#1 J-009610-06

Sense Sequence 5'ACGCUGAGGCCUACAGACAUU
 Antisense Sequence 5'PUGUCUGUAGGCCUCAGCGUUU

#2 J-009610-08

Sense Sequence 5'CCAAGAAGCGCCUGAUUGUUU
 Antisense Sequence 5'PACAAUCAGGCGCUUCUUGGUU

#3 J-009610-05

Sense Sequence 5'GGACAGGCCACUACCUAUGUU
 Antisense Sequence 5'PCAUAGGUAGUGGCCUGUCCUU

#4 J-009610-07

Sense Sequence 5'GCUGGUGGCUUUAUGGUGGUU
 Antisense Sequence 5'PCCACCAUAAAGCCACCAGCUU

We also obtained a control siRNA sequence that does not match any known gene sequence in GeneBank. This sequence was designated as C. (Dharmacon RNA Technologies ON-TARGETplus siCONTROL Non-targeting siRNA).

C D-001810-01-05

Sense Sequence	5'UGGUUUACAUGUCGACUAA
Antisense Sequence	3'ACCAAUUGUACAGCUGAUU

Transient Transfection of Dharmacon siRNA into U87-MG

The U87-MG cell line is a cultured human glioblastoma/astrocytoma cell line obtained from ATCC (ATCC number HTB-14). This cell line was chosen because it grows very nicely in cell culture and is tumorigenic when stereotactically injected into nude mouse or rat brain. We created a 24-well plate with cultured U87-MG cells plated at a density of 100,000 cells per well at the start of transfection. Our cultured cells grew in DMEM-F12 media with 10% fetal bovine serum, 1% L-glutamine, 1% penicillin/streptomycin, and 14 millimolar sodium bicarbonate, pH = 7.5. Our cells incubated at 5% CO₂ and 37° C.

We then prepared our stock solutions of siRNA using 5x siRNA buffer to a final concentration of 20 µM. We used a siRNA transfection kit (Ambion *Silencer* siRNA Transfection Kit, catalog # 1630 siPORT amine) to transfect our U87-MG cells (via liposome mediated transfection) with either #1, #2, #3, #4, or C siRNA. After incubation we created cell lysates by adding 1 cc of lysis buffer (50 mM pH 7.5 sodium phosphate, 10 mM, 10 mM 1-thioglycerol, 0.1% Triton X-100, and 1% NP-40) to our washed cell culture plates, scraping off the cells adherent to the plates, and homogenizing through pipetting. After this we quantified the protein in our lysates using the Bradford assay for protein concentration (absorbance at 595 nanometers). 10 µl of our cell lysates were combined with 990 µl of water, creating a 100-fold dilution. 400 µl of this dilution were then combined with 0.4 cc of water and 0.2 cc of Bradford coomassie blue dye (Bradford, 1976). We then ran the lysates on an SDS-polyacrylamide gel (10%) at 20

µg of protein/lane using the Bio-Rad mini-protean system. This gel was then equilibrated in 25 ml 1X CAPS buffer (10 mM CAPS, pH = 11 with 10% methanol) with 10% methanol and transferred onto a PVDF membrane at 100 V/1 hour. The membrane was then allowed to air dry, then wet with 100% methanol and then equilibrated in TBST (TBS-Tween: 10 mM Tris, Ph = 7.5; 150 mM NaCl; 0.05% Tween-20) for 5 minutes. We then blocked the membrane for 1 hour in TBST + 5% milk. A western blot was then performed to assay GATA-1 concentration using our antibody against GATA-1 (Santa Cruz Biotechnology, Inc. GATA-1 (H200): sc-13053) and a chemiluminescent secondary antibody (HRP-conjugated) against the primary antibody.

After chemiluminescence and development, encouraging results were obtained. Western blots obtained here showed the knockdown of GATA-1 protein very nicely. Upon further analysis we determined that #4 was the most efficient siRNA against GATA-1. After this experiment we utilized “quantum dots,” specialized our PVDF membranes in preparation for quantum dot blots. For this method, we washed our membrane 4 times after transfer (in CAPS buffer, water, methanol, and then water molecules bound to secondary antibodies that give off light when stimulated by certain wavelengths (Figure 19). There were significant differences in the way we developed again.) The biotinylated molecular weight marker strip was cut from the main blot and developed separately. The membranes were then washed in TBST and then blocked for 1 hour in 100% fish serum. Our primary antibody was then added to the blots (16 µl of primary antibody + 16 ml TBST with 25% fish serum for the main blot) and incubated for 1 hour and then washed twice in TBST with 25% fish serum followed by our secondary antibody (16 µl secondary antibody in 8 cc TBST/25% fish serum for primary

blot). We then concluded that siRNA sequence #4 is the most effective down-regulator of GATA-1 transcription in U87-MG cells (Figure 16). This was to serve as our sequence of choice for the next step in the experiments: to engineer an inducible glioma cell line able to produce siRNA against GATA-1 upon our command.

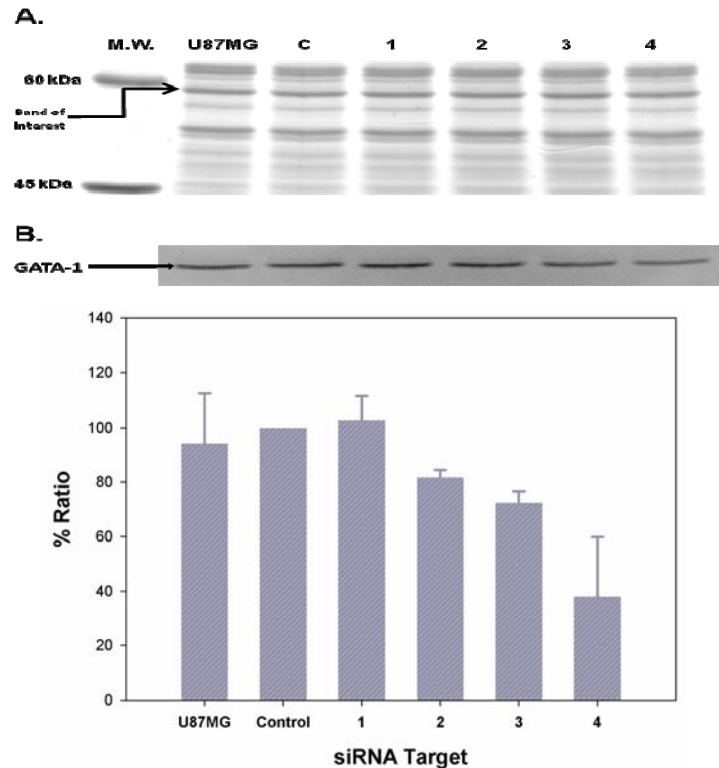


Figure 16: Representative Coomassie blue stain of SDS-PAGE gel (A) and western blot (B) against GATA-1 protein in U87-MG cells transfected with siRNA against GATA-1 mRNA transcripts: The knockdown levels of GATA-1 indicate that siRNA #4 is the most effective sequence at silencing GATA-1 protein expression. Averaged data from three independent experiments are shown; Average drop in GATA-1 expression = 62% \pm 21.6; $p = 0.008$. Data analysis was done in collaboration with Michael Monterey and Dr. Mathupala. The pixel density of western blots were calculated with Un-Scan-It digitizing software (Silk Scientific, Orem, UT). Data were tabulated with SigmaPlot 8.0 software (SPSS Inc., Chicago, IL). Band of interest; protein band used to normalize total protein in each lane. The Control was arbitrarily adjusted to 100% expression.

Long-Term Regulated Silencing of GATA-1: Tet-on/Tet-off System

Transfection of U87-MG cells with mobile genetic elements such as plasmids is much more efficient if a virus is used as a vehicle (i.e. transformation) rather than a

liposome. The next phase in our research involved engineering a virus in order to create a double stable tetracycline U87-MG tumor cell line containing 2 plasmids: A regulatory plasmid that produces a transcriptional activator in the presence of tetracycline (or doxycycline) and a response plasmid that responds to that transcriptional activating factor and produces siRNA against GATA-1. Both of these plasmids are available from various companies, and all plasmids are not created the same. The response plasmid is made as a circular piece of DNA containing several genes of interest to the researcher. These genes may include, among other things: Antibiotic resistance genes for cell selection after transfection or transformation, viral packaging genes for production of infectious virus to initiate transformation, a multiple cloning site (MCS) with specific restriction sites that the researcher may use enzymes to cut and insert a gene of interest into, and various promoters that control the genes on the plasmid (Figure 17).

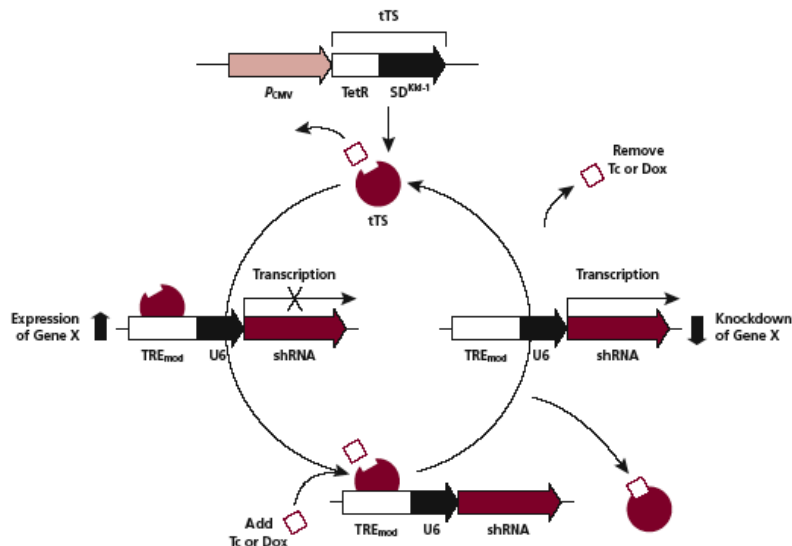


Figure 17: Schematic of gene regulation in the inducible tTS system. The suppressor tTS binds the *tetO* sequence in the TRE(mod) promoter region of the response plasmid, suppressing shRNA expression. In the presence of doxycycline or minocycline, the tTS dissociates from the TRE(mod) and allows activation of shRNA transcription from the downstream U6 promoter. [From the “Knockout Inducible RNAi Systems User Manual”, Clontech Laboratories, Inc.]

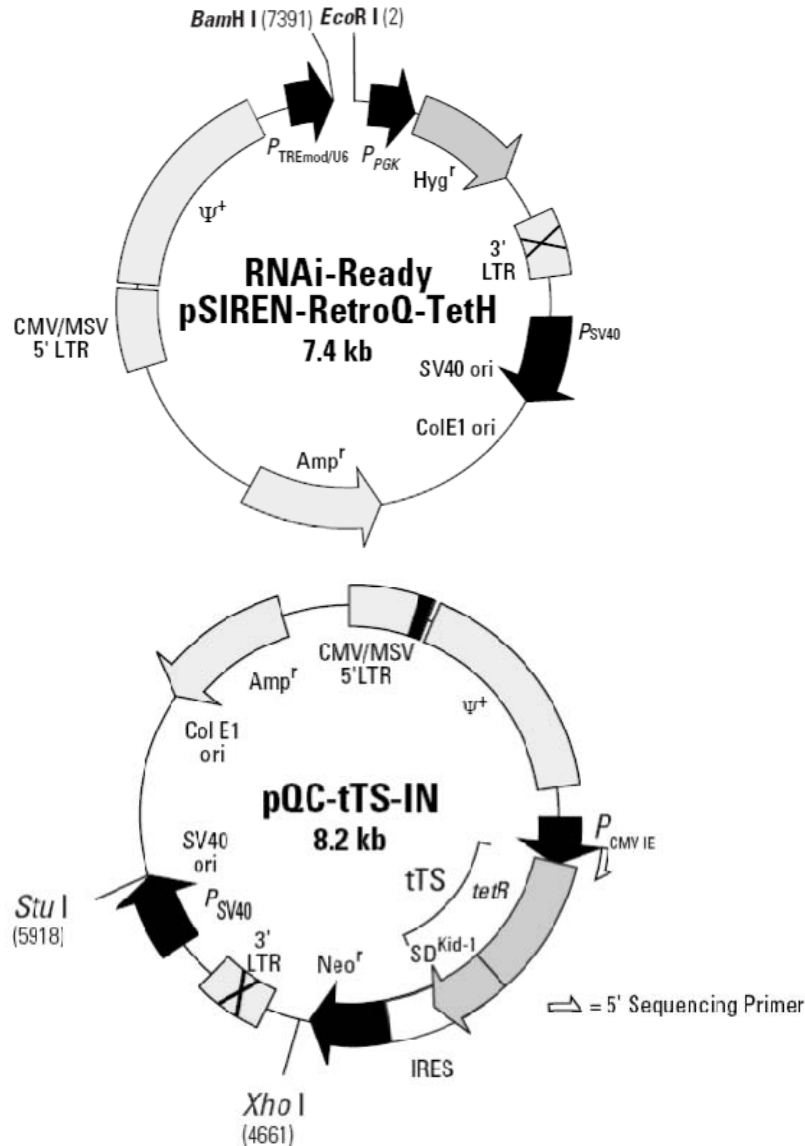


Figure 18: pQC-tTS-IN regulatory plasmid and RNAi-Ready pSIREN-RetroQ-TetH Response Vector (Clontech, PT3811-5, cat # 630925). The regulatory plasmid has a strong promoter (*P_{cmv IE}*) and ampicillin, G418 resistance genes. The response plasmid is roughly 1 kilobase smaller than our first response plasmid. It has no cGFP gene, so it must be selected for by the hygromycin resistance gene.

Our first step was to select a regulatory and response plasmid system, and we chose the BD Tet-on system (Figure 18). This vector's MCS had specific restriction sites, so we had to design forward and reverse sequence primers (oligonucleotides) for

GATA-1 siRNA and a forward sequencing primer specific for the cassette restriction sites.

PRIMER SET FOR CONTROL [CLONTECH]

FORWARD PRIMER

5'GAT-CCG-TTA-GTC-GAC-ATG-TAA-ACC-ATT-GAT-ATC-CGT-GGT-TTA-CAT-GTC-GAC-TAA-TTT-TTT-CCA-AG 3'

REVERSE PRIMER

5'AAT-TCT-TGG-AAA-AAA-TTA-GTC-GAC-ATG-TAA-ACC-ACG-GAT-ATC-AAT-GGT-TTA-CAT-GTC-GAC-TAA-CG 3'

PRIMER SET FOR SIRNA TEMPLATE #4 [CLONTECH]

FORWARD PRIMER

5'GAT-CCG-CCA-CCA-TAA-AGC-CAC-CAG-CTT-GAT-ATC-CGG-CTG-GTG-GCT-TTA-TGG-TGG-TTT-TTT-CCA-AG 3'

REVERSE PRIMER

5'AAT-TCT-TGG-AAA-AAA-CCA-CCA-TAA-AGC-CAC-CAG-CCG-GAT-ATC-AAG-CTG-GTG-GCT-TTA-TGG-TGG-CG 3'

U6 FORWARD SEQUENCING PRIMER

5'CTT-GAA-CCT-CCT-CGT-TCG-ACC-CCG-CCT-C 3'

We were then able to locate in this long sequence the area in which the siRNA #4 against GATA-1 is directed. Using this information, we then were able to design our control and test inserts (oligonucleotide sequences) to place into our plasmids. Since we knew the restriction sites on the plasmid (*Eco R1* and *Bam H1*) we were then able to design our primers (Integrated DNA Technologies). Once we received the single stranded control and test primers, we set up an annealing reaction to ligate the complementary strands together to form our cassettes. The primers were designed to

have overhanging ends that matched up with the restriction sites in the MCS. The cassettes do not ligate end-to-end with each other because the 5' ends are not phosphorylated (Figure 19).

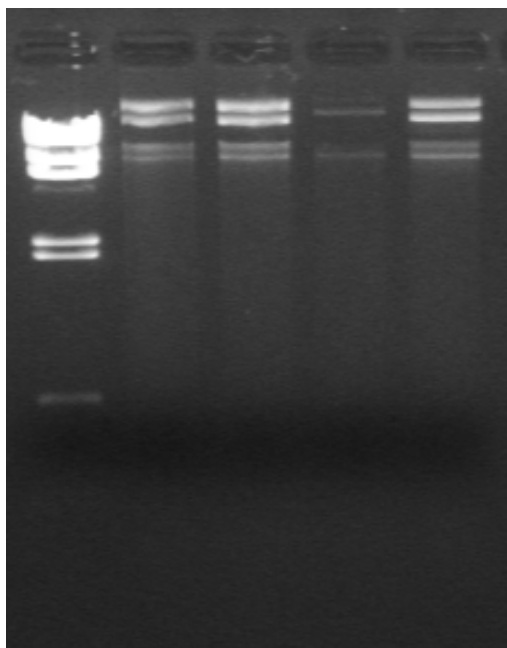


Figure 19: 0.8% Agarose DNA gel demonstrating our plasmids in their native, uncut state. The doublet represents the nicked and supercoiled states of the plasmids. Doublets representative of e.coli SURE. Lane MW = molecular weight marker

After application of specific restriction enzymes to the response plasmid, the plasmid is now opened at the MCS and is linear. Addition of our double stranded oligos initiated an annealing reaction and the plasmids now took up our cassettes into their MCS. We then placed our newly annealed plasmids (with our siRNA gene insert) into *E.coli* SURE cells by electroporation. These *E. coli* cells were then grown on ampicillin media (bacteria that have the plasmid are now ampicillin resistant, due to the gene on the plasmid). Once the plasmid has amplified in *E. coli* sufficiently, we used a Qiagen kit (Qiaprep) to isolate the plasmids from the e. coli cells. 3 ml of our overnight e.coli

cultures were spun down at 10,000 rpm x 2 minutes (1.5 cc per 1 minute, removing supernatant in between spins). We then added 150 µl of cold buffer P1 with RNase, resuspending the pellet. We then added 250 µl of buffer P2, then 350 µl of buffer N3 followed by centrifugation at 13,000 rpm at 4° C for 10 minutes. The supernatant was then recovered and centrifuged in a QIAprep spin column at 10,000 rpm for 30 seconds, followed by Buffers PB, PE, and EB with centrifugation between each steps. This sample was quantified in a spectrophotometer (260 nanometers) and run on an agarose gel. Afterwards, our plasmid was sent for DNA sequencing, which confirmed that in at least 1 set of plasmids, our cassette had been inserted. We then proceeded to place our plasmids into packaging cells (eukaryotic PA317 cells) via transfection. The goal of this step is to allow the plasmid to begin making virus, as our packaging cells are specially engineered to have the other half of the viral genome that is found on our response plasmid.

72 hours after transfection the culture supernatant was recovered from the culture tubes, centrifuged at 5000G for 5 minutes to sediment cell debris. Then 200 µl of supernatant was used on U87-MG cells permanently transfected with tTS in a 60 mm plate with 5 ml of DMEM medium (Polybrene was used to enhance transduction efficiency). 24 hours post transduction, the cells were selected in hygromycin and then trypsinized, plated onto a large 100 mm diameter plate and allowed to grow for 2 weeks until clonal cell populations appeared. Single clones were isolated using cloning cylinders (agarose based anchoring method)(Mathupala and Sloan, 2009). Then 6 individual clones were placed in individual wells in a 6 well plate (x µg/ml) doxyxycine and incubated for 2 days. A western blot was performed to determine the optimum

concentration of doxy required for GATA-1 knockdown.

SDS-PAGE and Western Blot for GATA-1 after Doxycycline and Minocycline Mediated Induction

Now that we have established our permanent transformed inducible U87-MG cell line and verified that both our response and regulatory plasmids have incorporated into the cell genome, we set up an induction experiment to verify that doxycycline and/or minocycline induces siRNA against GATA-1 transcripts and knocks down the level of this protein in our cells (and also to determine the optimum concentration of both drugs needed to achieve this).

We began by growing our transformed U87-MG cells in 6 well plates in DMEM without antibiotics. Stocks of doxycycline and minocycline (Sigma) were made at 1 mg/ml and pH = 7.4. We then added doxycycline and minocycline separately to two separate cultures in 6-well plates to create an increasing concentration of doxycycline and minocycline in each well as follows (in micrograms of drug/ml media): well 1 = 0, well 2 = 0.001, well 3 = 0.01, well 4 = 0.1, well 5 = 1, and well 6 = 10. The plate was incubated for 2 days and the cells were then washed with PBS, trypsinized, and made into cell lysates. We ran a western blot on these lysates with our primary anti-GATA-1 antibody, and our results demonstrated a significant knockdown of GATA-1 protein in the cells exposed to 10 μ g/ml of doxycycline and minocycline. We then repeated the experiment using a different, stronger serial dilution of doxycycline and minocycline (in μ g of drug/ml media): well 1 = 0, well 2 = 2.5, well 3 = 5, well 4 = 7.5, well 5 = 10, and well 6 = 20. In both the minocycline and doxycycline experiments we saw a significant knockdown of GATA-1 in the 10 and 20 μ g/ml wells (Figures 20, 21, 22, and 23)

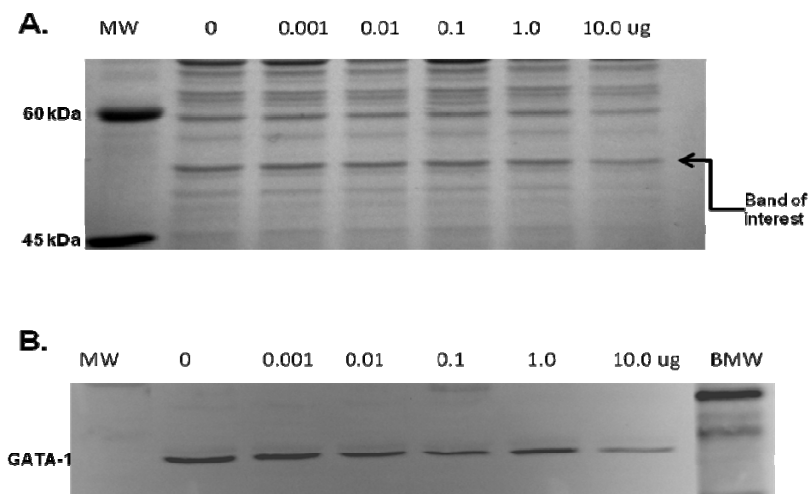


Figure 20: Coomassie blue stain of SDS-PAGE gel (A) and Western blot using Qdot and anti-GATA-1 primary antibody (B). Doxycycline induction of the response plasmid integrated into our U87-MG test cells with our siRNA #4 against GATA-1 indicated by concentration (0-10 μg doxycycline/ μg media). Protein concentration is equal in all lanes. MW = molecular weight marker, BMW = biotinylated molecular weight marker. Band of interest; protein band used to normalize protein content across samples.

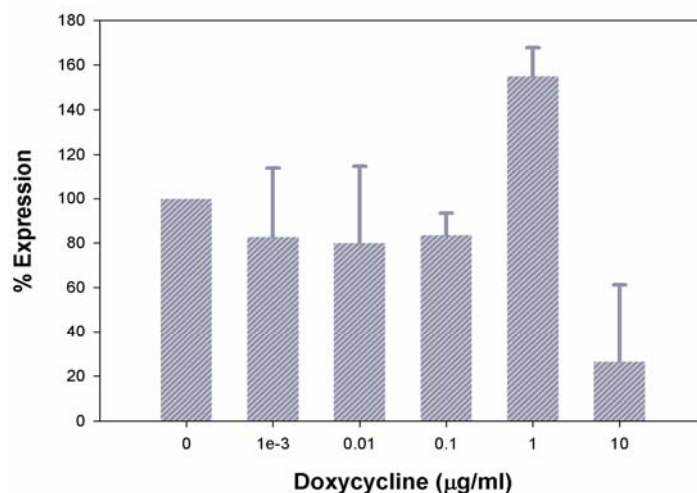


Figure 21: Quantification of doxycycline induction of shRNA against GATA-1. Downregulation of GATA-1 by doxycycline induction of siRNA against GATA-1 is evident from the decreased protein concentration of GATA-1 at 10 micrograms per milliliter. Averaged data from two independent experiments are shown; Average drop in GATA-1 expression = $73.5\% \pm 34.6$; $p = 0.095$. Data analysis was done in collaboration with Michael Monterey and Dr. Mathupala. The pixel density of western blots were calculated with Un-Scan-It digitizing software (Silk Scientific, Orem, UT). Data were tabulated with SigmaPlot 8.0 software (SPSS Inc., Chicago, IL). Band of interest; protein band used to normalize total protein in each lane. The 0 $\mu\text{g/ml}$ sample was arbitrarily adjusted to 100% expression.

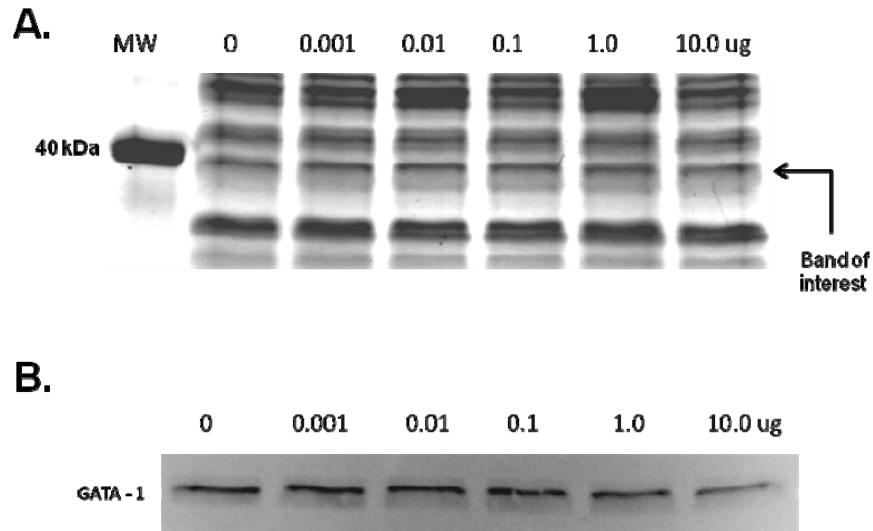


Figure 22: Coomassie blue stain of SDS-PAGE gel (A) and Western blot using Qdot and anti-GATA-1 primary antibody (B). Minocycline induction of the response plasmid integrated into our U87-MG test cells with our siRNA #4 against GATA-1 indicated by concentration (0-10 μg minocycline/ μl media). Protein concentration is evidently identical in all of the lanes. MW = molecular weight marker, BMW = biotinylated molecular weight marker.

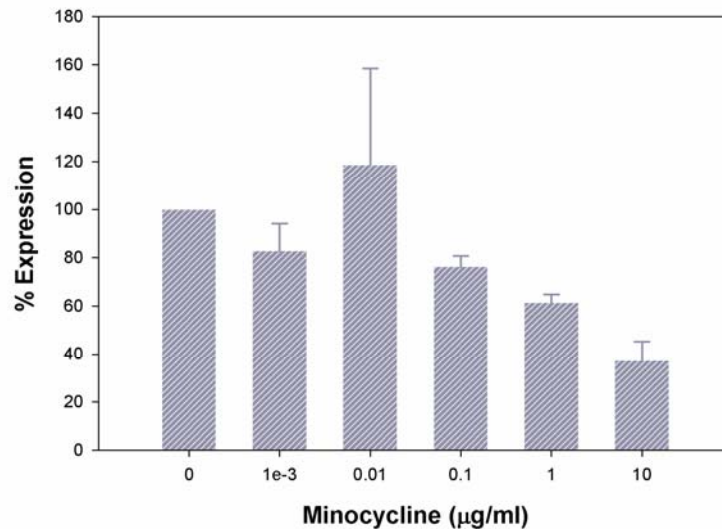


Figure 23: Quantification of minocycline induction of shRNA against GATA-1. Downregulation of GATA-1 by minocycline induction of siRNA against GATA-1 is evident from the decreased protein concentration of GATA-1 at 10 micrograms per milliliter. Averaged data from two independent experiments are shown; Average drop in GATA-1 expression = $62.8\% \pm 8.06$; $p = 0.008$. Data analysis was done in collaboration with Michael Monterey and Dr. Mathupala. The pixel density of western blots were calculated with Un-Scan-It digitizing software (Silk Scientific, Orem, UT). Data were tabulated with SigmaPlot 8.0 software (SPSS Inc., Chicago, IL). Band of interest; protein band used to normalize total protein in each lane. The 0 $\mu\text{g/ml}$ sample was arbitrarily adjusted to 100% expression.

Western Blot Analysis of both GATA-1 and MCT-2: Decrease in Levels of MCT-2 seen Concomitantly with Down-Regulation of GATA-1

The next logical step in our examination of GATA-1 is to determine the effect of decreased levels of GATA-1 on levels of MCT-2 in transformed U87-MG glioblastoma cells. If GATA-1 is responsible for upregulation of MCT-2 transcription and expression, then a decrease in levels of GATA-1 protein in our transformed tumor cells should lead to a decrease in levels of MCT-2 (although perhaps not in direct parallel).

We began by selecting 4 control and 4 test insert clonal isolates. Based on our induction data, we induced all 8 with 10 µg /ml doxycycline for 3 days. We then made cell lysates from all of the cultures and quantitated the protein in the previously described manner. We ran all 8 isolates on an SDS-PAGE gel at 20 µg of protein/lane and transferred it on to a PVDF membrane using our standard method previously described. We then probed our membrane with our primary antibody against GATA-1, applied secondary quantum dot antibody, and imaged the blot. We then re-probed the blot using our primary antibody against MCT-2 (Alpha Diagnostic International, Inc., San Antonio TX), re-exposed the membrane to our same quantum dot secondary antibody, and imaged the blot. The nature of quantum dot technology allows our primary and secondary antibodies to give off signal for a much longer time than standard HRP-mediated chemiluminescence allows, so multiple probes and images of the same blot are possible without loss of signal. The specific bands on the image were scanned using densitometric software (Un-Scan-It, Silk Scientific, Orem, UT). There are clearly changes in perceived levels of each protein due to background staining, and the quantitative data are presented as-is. A coomassie blue stain was performed on the original gel and verified that equal protein was used in each lane (Figures 24, 25, 26).

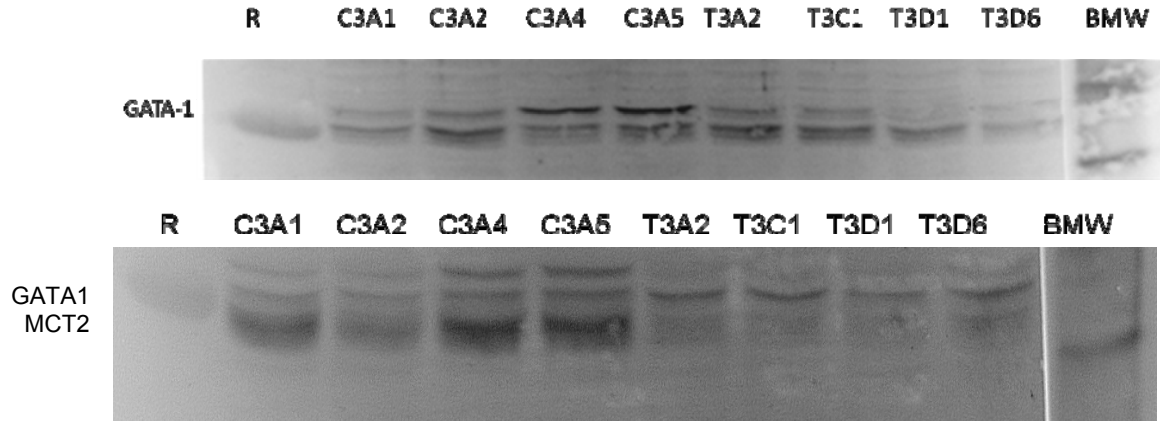


Figure 24: Western blot of control (labeled “C”) and test (labeled “T”) clonal isolates double probed for GATA-1 protein and MCT-2 protein. GATA-1 runs at 47 kDa whereas MCT-2 runs from 35-40 kDa, (since it is a membrane protein it runs faster than its estimated true weight of 55 kDa). Coomassie blue stained gel confirmed equal protein in all lanes. 20 μ g of protein were loaded in all lanes. The upper panel indicated the same western blot first probed with antibody against GATA-1 only, to differentiate between the two proteins.

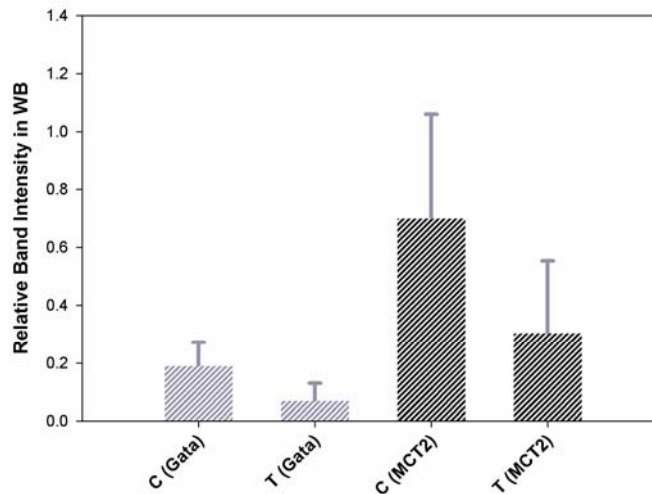


Figure 25: Densitometric results of the GATA-1 band using Un-Scan-It (Silk Scientific, Orem UT). C (Gata) corresponds to Lanes C3A1, C3A2, C3A4, C3A5 in the western blot; T (Gata) corresponds to T3A2, T3C1, T3D1, T3D6. For statistical analysis, the four individual control or test samples were analyzed for total protein and GATA-1 protein levels. Averaged data from each of the four individual control or test lanes are shown; Average drop in GATA-1 expression = 62.1% \pm 6.74; $p = 0.047$. Data analysis was done in collaboration with Michael Monterey and Dr. Mathupala. The pixel density of western blots were calculated with Un-Scan-It digitizing software (Silk Scientific, Orem, UT). Data were tabulated with SigmaPlot 8.0 software (SPSS Inc., Chicago, IL). Band of interest; protein band used to normalize total protein in each lane.

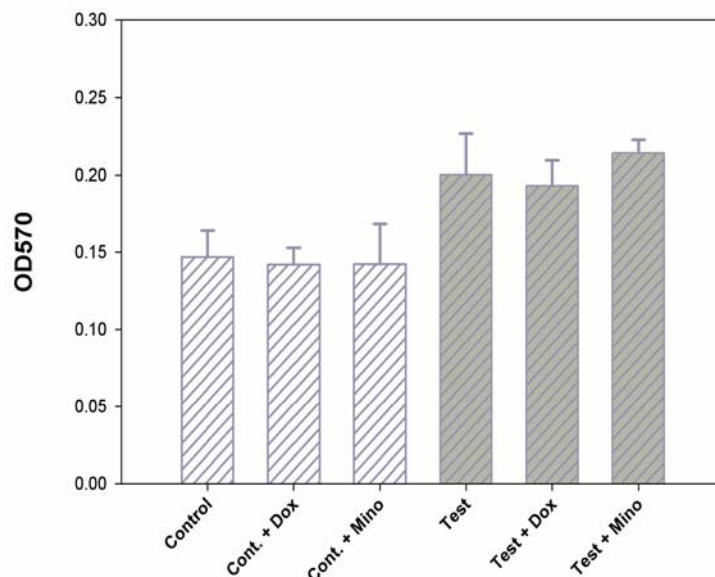


Figure 26: Densitometric results of the MCT-2 band using Un-Scan-It (Silk Scientific, Orem UT). The C (MCT2) and T (MCT2) correlate to the same respective lanes in the lower western blot. For statistical analysis, the four individual control or test samples were analyzed for total protein and MCT2 protein levels. Averaged data from each of the four individual control or test lanes are shown. Average drop in MCT2 expression = $56.5\% \pm 30.2$; $p = 0.1175$. Data analysis was done in collaboration with Michael Monterey and Dr. Mathupala. The pixel density of western blots were calculated with Un-Scan-It digitizing software (Silk Scientific, Orem, UT). Data were tabulated with SigmaPlot 8.0 software (SPSS Inc., Chicago, IL). Band of interest; protein band used to normalize total protein in each lane.

MTT Assay for Cell Proliferation

To test for effects of GATA-1 silencing, the engineered U-87MG cells were plated in DMEM media lacking phenol-red, in 24-well plates at 0.3×10^6 cells per well. Post 72 hrs plating, the media were aspirated and fresh pre-warmed media containing MTT at 0.5 mg/ml, according to established protocols (Freshney, 2005). The cells were incubated for 90 minutes in the tissue culture incubator until formazan formation was complete, and the medium aspirated out. 0.4 ml of DMSO was added to each well to dissolve formazan crystals and then pH adjusted for dye measurement by adding 100 μ l of Sorensen's glycine buffer (0.1M glycine, 0.1 M NaCl, pH 10.5). 100 μ l aliquots were

transferred to 96-well ELISA plates and the O.D. of each well measured at 570 nm in a Tecan Infinite M200 plate reader (Figure 27).

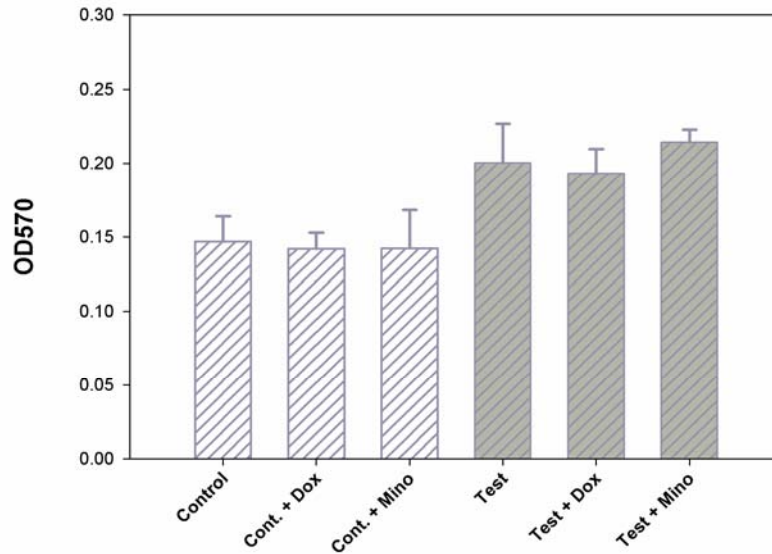


Figure 27: MTT assay data of proliferative rate between Test (GATA-1 siRNA) and Control (scrambled siRNA) cells: Doxycycline or minocycline treatments did not show statistically significant changes. The experiments were carried out 2 weeks after establishment of cell clones. A repeat study with well established clonal isolates (2-3 month) may be necessary to evaluate the efficacy of this tet-regulated induction system both *in vitro* and *in vivo*. Due to time constraints we could not complete these studies, but are planned as future research (we may utilize more advanced tet-regulated systems that have been introduced by several biotechnology companies during the last year). Averaged data from each of the six individual control or test lanes are shown; Average decrease in proliferative rate (Control - Doxycycline) = 3.20% ± 0.02; p = 0.35; (Control - Minocycline) = 3.13% ± 0.02; p = 0.56. (Test - Doxycycline) = 3.60% ± 0.02; p = 0.68; In contrast, an increase in proliferation was seen for minocycline treated test cells; (Test - Minocycline) = 6.88% ± 0.02; p = 0.00. Data analysis was done in collaboration with Michael Monterey and Dr. Mathupala. Data were tabulated with SigmaPlot 8.0 software (SPSS Inc., Chicago, IL).

CHAPTER 3

OVER-EXPRESSION OF GATA-1 IN GLIOBLASTOMA: AN *IN VITRO* STUDY

Introduction

In the previous chapter, our plan was to address the effects of silencing GATA-1 on proliferation of U87-MG glioma cells. Here, we have taken the opposite approach, i.e., overexpressing GATA-1 in the same line to test for the effects on cell proliferation, changes in metabolism related to glycolysis, i.e., lactate metabolism (efflux), and to test for influence of GATA-1 expression on MCT-2 promoter regulation. Based on the positive results we obtained for these objectives, we then proceeded to test the effects of GATA-1 over-expression on cell cycle progression in the glioma cells, which also yielded novel results.

Attempts to Over Express GATA-1 via Exposure of Glioma Cells to Erythropoietin (Epo)

Previous investigators have established that the Epo receptor is expressed in U-87MG glioma cells (Acs et al., 2001). Thus, our first attempt was to overexpress GATA-1 in the same cells by exposure of the cells *in vitro* to Epo. We obtained recombinant human Epo from Sigma chemical company and exposed U87-MG glioma cells growing under exponential culture conditions in both low glucose (5 mM) DMEM media as well as hi glucose (25 mM) DMEM/F12 media supplemented with either 1% or 5% FBS, to test for induction of GATA-1 upon exposure of the cells to Epo. In brief, the cells were exposed to between 0 to 10 pM Epo for 5 days in culture (Kitamura et al., 1989) and then cell extracts prepared as described in Chapter 2. 20 to 40 μ g of total protein were resolved on SDS-PAGE gel (10%), and western blotted with polyclonal antibody against GATA-1 (Novus Biologicals, CO). However, we could not see changes in expression in

any of the Epo/serum combinations that were tested by us (data not shown). Thus, we decided to take a molecular biological approach, where GATA-1 expression was driven by a strong viral promoter.

Overexpression of GATA-1 in U87-MG Cells via Transfection with a GATA-1 Expression Vector

In order to overexpress GATA-1 we obtained an expression ready GATA-1 clone from Invitrogen Inc. (GeneStorm Expression Ready Clone, in pcDNA 3.1 vector) (Figure 28). Plasmid DNA was prepared from *E. coli* DH5alpha harboring the vector by standard plasmid mini-prep procedures (Qiagen MiniPrep) and 2.5 µg of plasmid containing the GATA-1 expression cassette or naked pcDNA3.1 vector were transfected into U87-MG cells using Lipofectamine-2000 (Invitrogen) using standard procedure described in Chapter 2. The transfections were carried out in 60 mm tissues culture plates, and 24 hrs post-transfection, trypsinized and replated in 100 mm diameter plates in DMEM low-glucose medium supplemented with 100 µg/ml Zeocin as the selection antibiotic. The cells were maintained for two weeks with media changes every 3-days to select for cell clones. 6 each of individual clones were selected with cloning cylinders as described before (Mathupala and Sloan, 2009) and placed in 6-well plates. After further culture in Zeocin media, cell extracts were made with untransfected U-87MG, those transfected with pcDNA3.1 and with vector harboring GATA-1 expression cassette.

A nuclear extract from K-562 erythroleukemia cells (Active Motif, CA) was used as a positive control during western blotting, as these cells highly express GATA-1 endogenously.

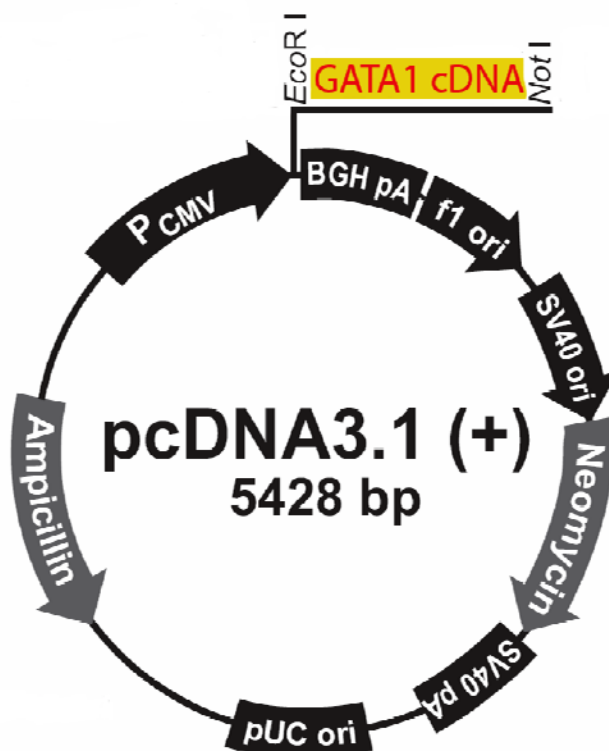


Figure 28: Schematic for GeneStorm expression ready GATA-1 clone vector (Invitrogen, Inc.) used to overexpress GATA-1 in our U-87MG cells. The Pcmv is a very strong viral promoter that constitutively expresses GATA-1 protein. Ampicillin was used to select for the plasmid in e. coli and G-418 (a neomycin analog) was used in mammalian cells (U-87MG)

As can be seen from the western blot method using Quantum Dots has been described in Chapter 2), the selected cell clone that harbored a GATA-1 expression cassette show clear overexpression of GATA-1, and this coincides with the GATA-1 band from the positive control (K-562 nuclear extract). Also, both the untransformed U87-MG cells as well as the control cells that harbor the naked pcDNA3.1 vector show similar levels of GATA-1 expression. Thus, the cell lines could be used in the following assays to test for biochemical changes in the cells due to GATA-1 (Figure 29).

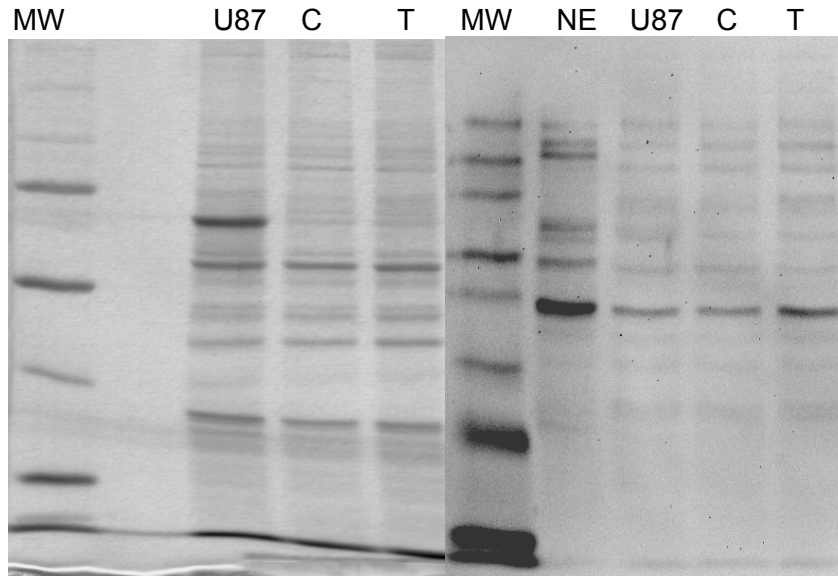


Figure 29: Coomassie blue dye of native SDS-PAGE gel (left) and western blot for GATA-1 protein (right) demonstrating overexpression of GATA-1 protein in test U-87MG cells harboring our expression ready GATA-1 plasmid. Increased GATA-1 correlates to our nuclear extract positive control. MW = molecular weight marker, NE = nuclear extract, U87 = U-87MG cell lysates, C = Control plasmid insert, T = Test plasmid insert.

MTT Assay for Cell Proliferation

To test for effects of GATA-1 overexpression, both control and test cells were plated in DMEM media lacking phenol-red, in 24-well plates at 0.3×10^6 cells per well. Post 72 hrs plating, the media were aspirated and fresh pre-warmed media containing MTT at 0.5 mg/ml, according to established protocols (Freshney, 2005). The cells were incubated for 90 minutes in the tissue culture incubator until formazan formation was complete, and the medium aspirated out. 0.4 ml of DMSO was added to each well to dissolve formazan crystals and then pH adjusted for dye measurement by adding 100 μ l of Sorensen's glycine buffer (0.1M glycine, 0.1 M NaCl, pH 10.5). 100 μ l aliquots were transferred to 96-well ELISA plates and the O.D. of each well measured at 570 nm in a Tecan Infinite M200 plate reader.

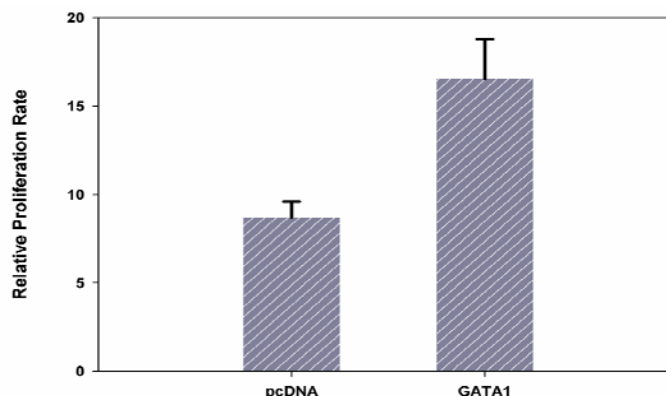


Figure 30: MTT proliferation assay of U87-MG cells transfected with either pcDNA containing vector (control) and GATA-1 containing vector (test). There is demonstrated a 1.9-fold increase in proliferation of the test U-87MG cells compared to the control group, indicating that GATA-1 overexpression enhances tumor cell proliferation.

The data were calculated in quadruplicate and indicate approximately 1.9-fold enhancement in proliferation with the GATA-1 overexpressed cell clone. Thus, the data indicate that overexpression of GATA-1 provides a significant advantage to tumors in enhancing their proliferation (Figure 30).

Cell Cycle Analysis

For this study, the cells were grown as above, in DMEM medium supplemented with 10% FBS, and the cells harvested in exponential culture by trypsinization. The cells were resuspended in the same media for the cells to recover from trypsin treatment, and then processed for cell cycle analysis by flow-cytometry.

We set up cultures of normal U-87MG cells, U-87MG cells transfected with the control plasmid, and cells transfected with our test plasmid that overexpresses GATA-1. Cells were harvested and counted to 1×10^6 density, then centrifuged at 1200 rpm for 5 minutes. The pellet was resuspended in 1 ml of 70% ethanol and fixed at 4°C for 30 minutes. The cell suspension was then respun at 2000 rpm for 5 minutes. The pellet was resuspended in 1 ml PBS and spun at 3000 rpm in refrigerated centrifuge. This

process was then repeated twice. 100 µl of 100 µg/ml RNase was added and incubated for 5 minutes. 400 µl of 50 µg/ml propidium iodide was then added and the samples were run through the flow cytometer with a 488 nm light source triggered on the propidium iodide signal. Samples were first gated by forward scatter against right angle light scatter (Figures 31, 32, 33, 34).

The large population of cells in both diploid and tetraploid states may reflect the extremely aggressive nature of these tumors. Perhaps the most alarming fact is that GATA-1 overexpression leads to a greater population of already extremely malignant cells (namely, wild-type U-87MG) to enter states that may make them even more malignant, in that these tumor cells are now more adept at survival in highly unfavorable intratumoral environments (Castedo et al., 2006).

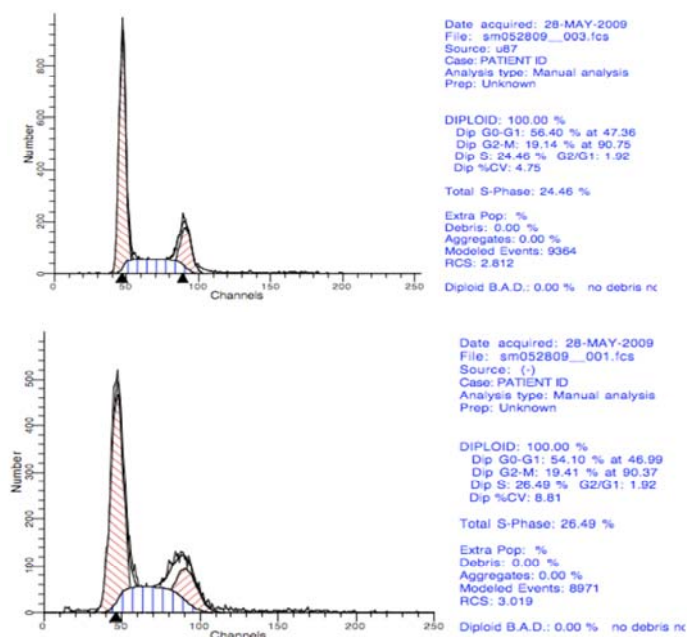


Figure 31: Diploid cell cycle analysis from flow cytometry data for normal U-87MG cells (above) and cells transfected with our control plasmid (below). There is not much difference between the control and wild type cell populations with regard to diploid populations, ensuring that the control plasmid did not affect the cell cycle and is therefore a good control.

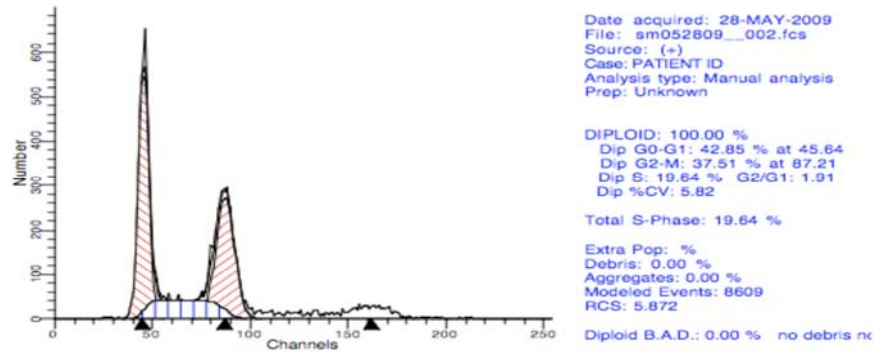


Figure 32: Diploid cell cycle analysis from flow cytometry data for U-87MG cells transfected with our GAT-1 overexpression plasmid. There is a large increase in the diploid population of cells in this group as shown by the second red peak. Furthermore, there is a tetraploid peak at 160. This demonstrates that GATA-1 overexpression has a positive effect on cell survival and resists programmed cell death.

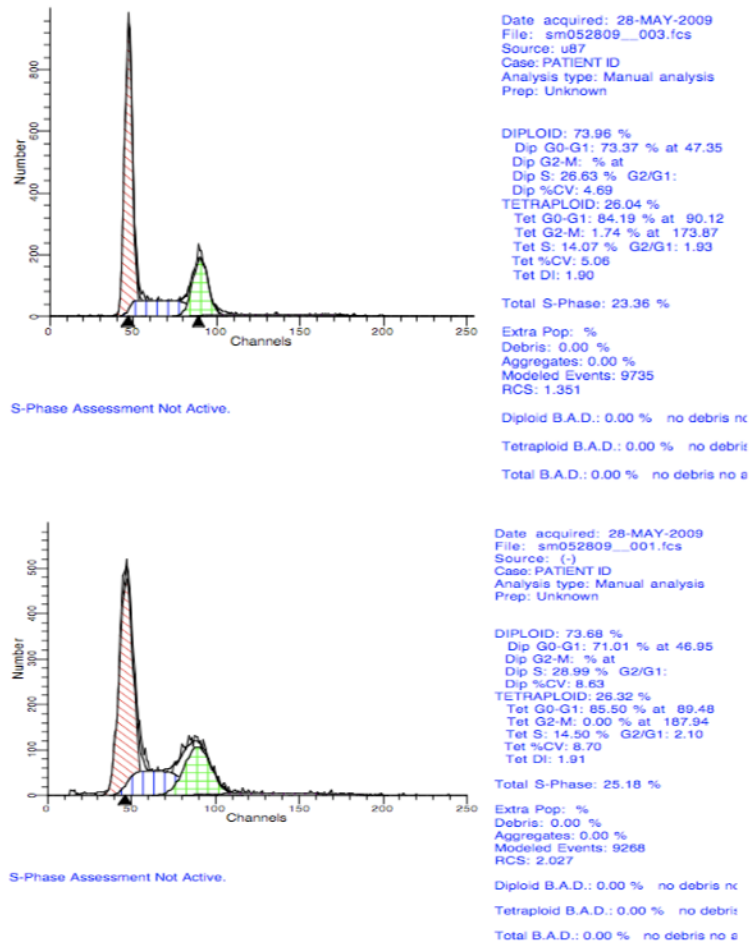


Figure 33: Tetraploid cell cycle analysis from flow cytometry data for U-87MG cells transfected with our GAT-1 overexpression plasmid. Again seen here is the large increase in the diploid population of cells in this group, demonstrating that GATA-1 overexpression has a positive effect on cell survival and resists programmed cell death.

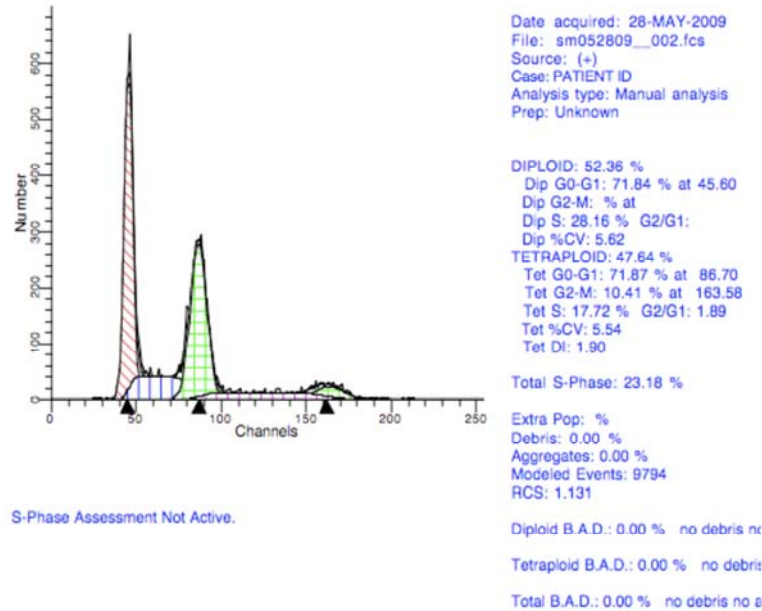


Figure 34: Tetraploid cell cycle analysis from flow cytometry data for U-87MG cells transfected with our GATA-1 overexpression plasmid. The tetraploid peak is apparent here (furthest right green peak), indicative of rampant cell proliferation. This is especially alarming because this may be a sign of increasing aggressive behavior of these already malignant tumor cells.

Lactate Efflux by GATA-1 Overexpressing U87-MG

This experiment was done to test whether the GATA-1 overexpressing cells have enhanced capacity for glycolysis, i.e., enhanced efflux of lactic acid, as this would support our hypothesis that GATA-1 promotes the malignancy of the tumor.

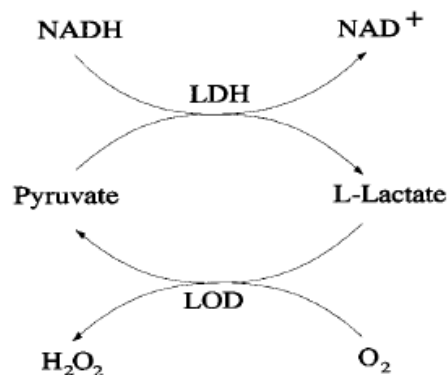


Figure 35: Schematic for enzymatic cycling assay for lactate using NADH/NAD⁺ absorbance. LDH = Lactate dehydrogenase; LOD = Lactate oxidase (microbial)

Thus, culture supernatants from cells grown in DMEM/F12 media supplemented with 10% FBS (a high glucose concentration was used to maximize the glycolytic flux across cells for this study) were harvested from both control and test cells, and subjected to analysis for lactate (Mathupala et al., 2004). In brief, 10 μ l aliquots of the supernatants (the culture medium was replenished 24 hrs before measurement so that the lactate that was accumulated since cells were plated was not assayed) were assayed for lactate using a cyclic assay system (Valero and Garcia-Carmona, 1996). The assay system consisted of 1.0 ml of the following; 0.94 ml of 50 mM Tris, pH 7.6, 2 μ l of lactate dehydrogenase (1U/ μ l) Sigma, lactate oxidase (0.25 U/ μ l), and beta NADH (3.6 mg/ml). The disappearance of NADH was measured at 340 nm to calculate the amount of lactate in the culture supernatant.

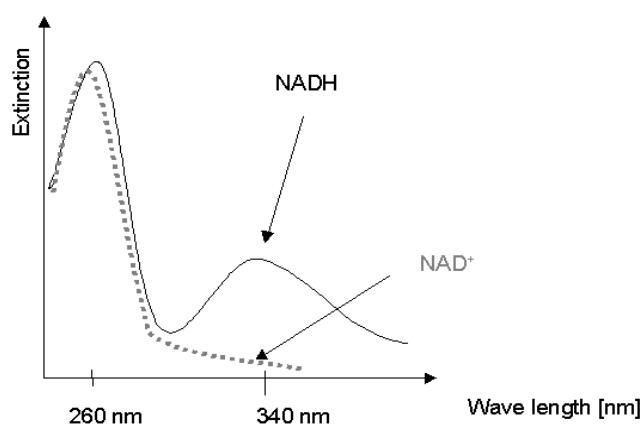


Figure 36: Assays done at 340 nm to detect loss of absorbance by NADH upon conversion to NAD⁺

The results here indicated an enhancement of lactate efflux of approximately 44% during the 24 hr period when the cells were cultured in DMEM/F12 media containing 25 mM glucose. Thus, a significant enhancement in lactate efflux was seen when GATA-1 was overexpressed, indicating a true physiological enhancement of glucose metabolism due to GATA-1 expression in these glioma cells. It is highly likely

that other metabolic routes, or the expression of other enzymes that are key to central metabolic pathways are also affected by GATA-1 overexpression, to impart such an increase in lactate efflux, as simply increasing MCT2 gene expression via GATA-1 may not, by itself, lead to such a pronounced increase in lactate efflux. The above result opens up additional avenues to investigate about the metabolic paths that may be central to glioma proliferation and survival.

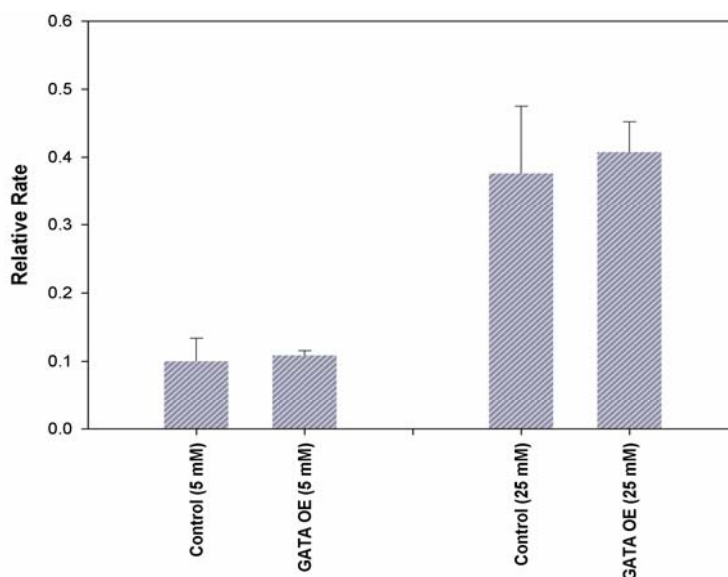


Figure 37: Lactate efflux rates of control and GATA overexpressed (OE) U-87MG glioma cells in high glucose DMEM/F12 media (25mM). The extracellular lactate levels were measured and divided by the cell count for each experiment to obtain the lactate-per-cell ratio. Values for the controls were arbitrarily adjusted to 1.00 (average of 6 experiments). The GATA-1 over-expressed cells showed a 1.44-fold increase in lactate efflux (1.44 ± 0.36 ; $p = 0.0140$). The cells were plated in 100 mm diameter tissue culture plates followed by a media change at ~ 50% confluency. The extracellular lactate was assayed 24-hrs later. Cells were then trypsinized and enumerated using a Coulter counter.

Luciferase Reporter Gene Analysis

For this study, the 4.2 kbp proximal promoter of MCT-2 (described in the introduction under Preliminary Data) was cloned into pGL2 Basic luciferase reporter gene vector (Figure X,.Promega, WI). In brief, the proximal promoter of MCT2 and part

of the first exon (untranslated region) were cloned into the multicloning site (MCS) of the pGL2-basic vector at the KpnI and Hind III sites (the KpnI site was available 5' to the promoter insert in the multicloning site of the original pUC18 clone of the promoter, while a Hind III site was available in the first exon of the MCT2 promoter).

For the cloning, both pGL2 basic vector and the pUC18 vector harboring the 4.2 kbp proximal promoter were cultured in *E. coli* SCS110 (methylation deficient) and plasmid isolated with Qiagen Plasmid MiniPrep kit. The plasmids were double digested with KpnI and Hind III (from New England Biolabs, using the recombinant plasmid was digested in NEB buffer 2, which is compatible with both enzymes). After a 2 hr digestion at 37°C, the digests were resolved by 0.8% agarose gel electrophoresis, and the primary bands (4.2 kbp for promoter and 5.6 kbp for pGL2-basic) were excised, and the DNA released by processing via Qiagen Qiaquick Gel purifications kit into 50 µl / 50 mM Tris, pH 8.5.

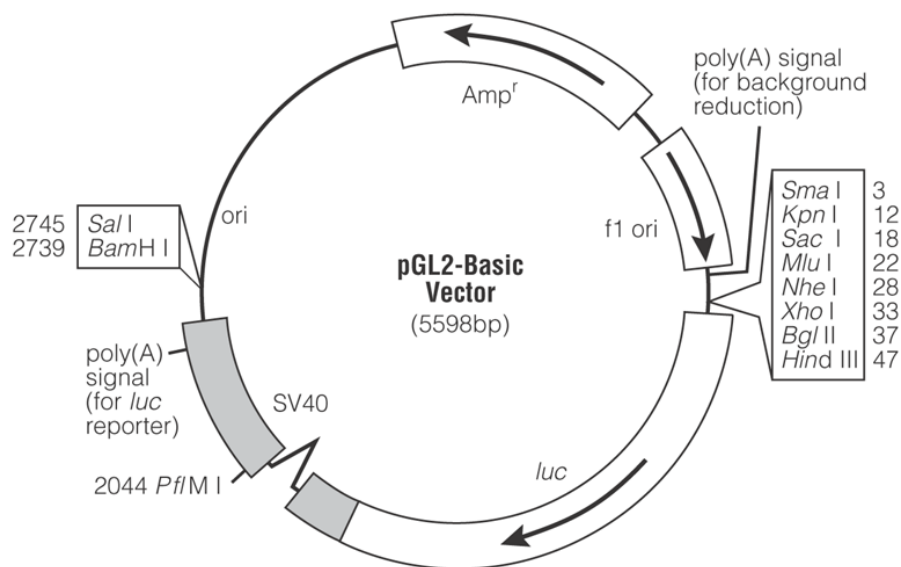


Figure 38: Reporter gene vector used for analysis of MCT-2 promoter activity from Promega.

3.5 μ l aliquots of each were ligated together in a 10 ml reaction volume with T4 DNA ligase (1 U) at 13 $^{\circ}$ C in an overnight incubation. 0.5 ml of the ligation was used to transform electrocompetent SCS110 *E. coli* cells using an Eppendorf 2510 electroporator (18,000 V/cm field strength), and the cells recovered in S.O.C. media for 1 hour. The cells were then plated in LB-ampicillin agar plates (50 μ g/ml ampicillin) and single colonies isolated after overnight incubation at 37 $^{\circ}$ C. Plasmid DNA was prepared from the clones as before using Qiagen Miniprep kits and insert verified by DNA sequencing.

Subsequently, nested deletion mutants were made of the luciferase reporter plasmid to generate a 3 kbp proximal promoter clone and a 2 kbp proximal promoter clone (made by Dr. Mathupala and clones isolated by Mr. Phil Benson). In brief, the MluI site on pGL2 Basic vector (resistant to digestion with Exonuclease III) and MluI site (sensitive to Exonuclease III digestion) was used to prepare the deletion mutants in a timed digestion reaction (Sambrook and Russell, 2001).

These plasmids, along with a control luciferase plasmid based on Renilla luciferase were used to test for promoter activation using the Dual-Glo luciferase Assay system according to the manufacturer's instructions. In brief, 1.2×10^6 U87MG glioma cells (either the control cells or, GATA-1 overexpressing cells) were first mixed with 1 μ g Renilla luciferase plasmid vector (this vector normalizes transfection efficiency across all reactions involving the MCT2 promoter-pGL2 basic vector based transfections in steps described below. Then, the mix was aliquoted into three, and 9 μ g equivalent of basic vector (with no promoter), the 3 kbp promoter, or the 2 kbp promoter was mixed into the individual aliquots. Equimolar amounts of the promoter was used in the

transfections. The transfections were completed in DMEM-Basal medium (no serum present), in the presence of lipofecamine-2000 under the same conditions described in Chapter 2, and plated into wells of a 24-well plate (5×10^4 cells per well; 8 wells per vector). 6 hrs post transfection, media in wells were changed to DMDM/F12 (phenol red free medium) supplemented with 10% FBS. 72 hrs post-transfection, the media was aspirated, and the cells lysed in lysis buffer (Dual Glo Luciferase reagent) provided by manufacturer (250 μ l per well), aliquoted 50 μ l per well in a white-wall 96-well plate and then assayed for firefly luciferase activity (bioluminescence setting, Tecan Infinite M200 plate reader). Subsequently, the firefly luciferase activity was quenched by a substrate/reaction condition change (Dual-Glo Stop and Glo Reagent) by adding 50 μ l to each well, and then assayed for Renilla luciferase, to normalize the transfection efficiencies across the three sets of experiments.

Then, the data were calculated by dividing the firefly luciferase reading with the reading for Renilla luciferase, to identify any changes in MCT2 promoter activation.

Based on the results we can see an approximate 3.3 fold activation is seen with the 2 kbp promoter while a 1.9 fold activation is seen with the 3 kbp promoter, thus clearly indicating promoter activation upon the presence of GATA-1. Furthermore, the results clearly correlate with the lactate assay studies described previously, proving our overall hypothesis of the involvement of GATA-1 in enhancing glioma metabolism and proliferation.

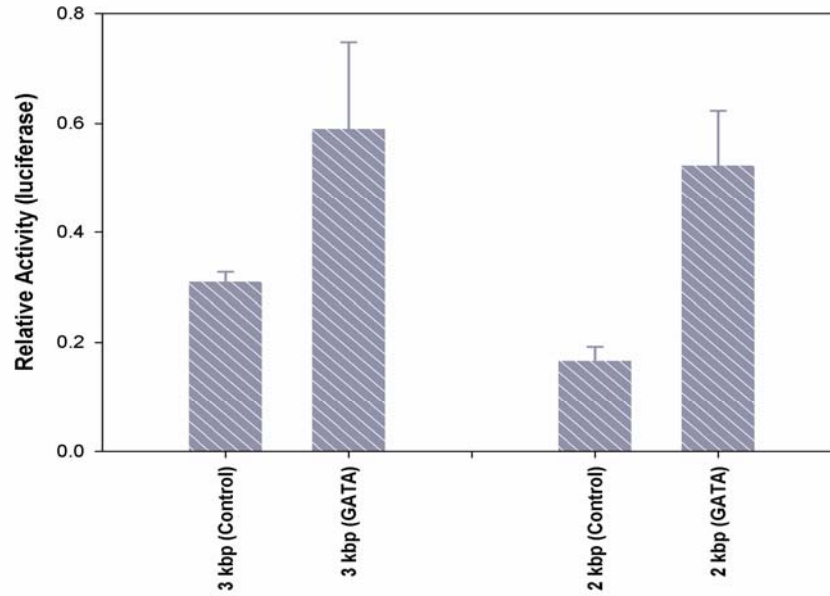


Figure 39: Reporter gene activation of two nested deletion mutants of the 4.2 kilobase pair proximal MCT-2 promoter. Two deletion constructs were used: one 3 kbp and the other 2 kbp. A 1.9-fold increase in promoter activity was seen for the 3 kbp proximal promoter region (1.9 ± 0.08 ; $p = 0.04$), while a 3.13-fold increase was seen for the 2 kbp proximal promoter region (3.13 ± 0.06 ; $p = 0.004$).

CHAPTER 4

CONCLUSIONS AND FUTURE DIRECTIONS

GATA-1 influences the Monocarboxylate Transporter-2 (MCT-2) Expression Resulting in Altered Glycolytic Capacity in GBM Cells

The overall goal of my thesis research was to elucidate whether changing the expression levels of GATA-1 in the model GBM cell line under study, U87-MG glioma, would in turn alter the MCT-2 expression levels (based on the presence of GATA-1 response elements on the proximal promoter of MCT-2, and to test whether this would have direct influence on the glycolytic flux across the GBM cells. It is primarily this metabolite flux that maintains the high proliferative capacity in malignant tumors and any changes to the flux should have a significant influence on the tumor growth *in vitro*, which would relate to any altered growth rate in an *in vivo* tumor model, or in a brain tumor patient.

We began our project by taking a closer look at GATA-1, a transcription factor that was previously believed to only participate in blood cell maturation before it was discovered to be present in very high levels in GBMs (both in cell culture and from *de novo* surgical specimens). We set out to examine what would happen to GBM metabolism and proliferation if levels of GATA-1 protein were decreased and increased. We used host cell machinery to degrade mRNA transcripts of GATA-1 using carefully chosen, most optimum shRNA against GATA-1. We selected this shRNA from a pool of 4 possible siRNA sequences specific only to the GATA-1 gene. We demonstrated through lipofection of U87-MG cell cultures that siRNA sequences were all successful at decreasing the levels of GATA-1 protein in these cells, and that sequence #4 was the most efficient one. We then engineered a stable U-87MG cell line (via virus-mediated

transformation) capable of producing shRNA against GATA-1 in response to administration of tetracycline to the media. We accomplished this by using the Clontech tet-on/off plasmid system. After down-regulating GATA-1, we examined the effect that this had on synthesis of MCT-2 in GBMs and on cell metabolism and proliferation.

The next phase of this work was, in essence, the opposite of the first. We used a different set of plasmid vectors to constitutively express GATA-1, thereby creating in our U-87MG cells a state of GATA-1 over-expression. We looked at several different aspects of GBM metabolism in these U-87MG cells, including the rate of lactate efflux through MCTs, cell cycle analysis, cell proliferation rates, and reporter gene analysis of the MCT-2 gene.

Long-term GATA-1 overexpression data presented in Chapter 3 showed significant enhancements in both glycolytic flux (lactate efflux) and MCT-2 expression (western blot analysis), as well as enhanced proliferation of GATA-1 overexpressing U87-MG cells (MTT assay), thus supporting our overall hypothesis. The observed high rate of lactate efflux may be due to GATA-1 influencing not only the levels of MCT-2 but other enzymes along the glycolytic pathway (yet to be identified as being modulated by GATA-1).

The overall goal of the project was to test whether we can inhibit the glycolytic rate of GBMs via RNAi mediated methods and if so, whether that would be applicable in an *in vivo* setting (animal model), and in a future clinical setting. The preliminary results from Chapter 2 indicate that RNAi mediated methods may not be sufficiently strong for complete silencing of GATA-1 expression, at least in the GBM model used, or perhaps

the engineered cells (with GATA-1 silenced) need to be tested for a longer period of time (multiple rounds of cell divisions).

An alternative method would be to inhibit GATA-1 via small molecule drugs, which are currently being developed by a pharmaceutical company in Japan (Kawa Co., Japan). These may be a suitable alternative to RNAi mediated silencing of GATA-1, or may be useful in combination therapies with other metabolic targeting small molecule drugs to inhibit GBMs.

The Influence of GATA-1 on Tumor Growth has already been Acknowledged by the FDA

As mentioned in the introductory chapter, GATA-1 plays a key role in erythrocyte development and maturation. GATA-1 knockout mice are unable to produce any mature red blood cells and production and maturation of other blood cells (including megakaryocytes, platelets, and eosinophils) is severely hindered. Recall, as well, that GATA-1 has been linked to anti-apoptotic proteins such as Bcl-_{XL}, cell cycle core components, the erythropoietin receptor, and other proliferative genes. When the NIH grant that the research is based on was first submitted in 2004, we proposed based on the preliminary studies outlined in Chapter 1 (preliminary data on GATA-1 overexpression in GBMs), that use of erythropoietin to treat anemia in brain tumor patients may be counterproductive, as it would lead to Epo dependent enhancement of GATA-1 levels in these tumor leading to more aggressive tumor growth.

This fact has now been acknowledged by the FDA in 2006, when they released a “black-box” warning on the use of Epo on patients with “head-and-neck” cancers. Thus, the clinical applicability of our studies on tumor patients is quite evident from such warnings (Figure 40).

Epogen
epoetin alfa

Black Box Warnings ⓘ

Increased Mortality and Serious Cardiovascular Events in CRF Pts
individualize dose to target Hgb 10-12 g/dL; incr. risk of death and serious cardiovascular events when administered to target Hgb >12 g/dL

Increased Mortality and/or Tumor Progression in Cancer Pts
use only for chemo-related anemia in pts where cure is not the anticipated outcome; increased mortality and/or risk of tumor progression or recurrence was seen in pts w/ breast, head/neck, lymphoid, cervical and non-small cell lung CA; to decrease these risks, as well as risk of serious cardio- and thrombovascular events, use lowest dose needed to avoid RBC transfusion, D/C once chemo course completed

Increased Thromboembolic Events in Surgery Pts
consider DVT prophylaxis due to incr. DVT rate in pts not receiving prophylactic anticoagulation

Figure 40: FDA black-box warning for Epogen (epoetin alfa) warning of the tendency of this drug to increase mortality of cancer patients and lead to accelerated tumor progression. Since erythropoietin has been shown to up-regulate GATA-1 levels during red blood cell maturation, one of the likely mediators of this phenomenon is GATA-1, likely up-regulated by the drug. (online.epocrates.com/u/10b2027/Epogen/Black+Box+Warnings)

Future Directions

As planned at the outset of my project, the *in vitro* studies outlined in the thesis will be expanded further to include RNAi studies on a long-term basis and then will be tested *in vivo* (RNAi mediated silencing and its effect on tumor proliferation) using the tet-regulated systems in an orthotopic nude rat model. We were unable to complete the *in vivo* studies due to both time constraints and technical difficulties at the time. Thus, the goal is to repeat those studies first *in vitro* using the same Tet-based system or alternate (more recent, upgraded) systems, and evaluate the effects of GATA-1 silencing on a long term basis *in vitro*, and then transfer the experimental system to an *in vivo* nude rat model for long term studies.

As discussed earlier, small-molecule drug candidates are under development (GATA-1 antagonists), and if these become available for preclinical studies they can also be tested in parallel with our other future studies outlined above.

In conclusion, our finding that GATA-1 is overexpressed in GBMs was novel, and paves the way for an addition to be made to the repertoire of currently available therapeutics in use against brain tumors in a future clinical setting. The research that was concluded in the thesis project clearly indicates a direct correlation between this transcription factor, formerly known to be only involved in erythropoiesis, and glycolysis, a key metabolic pathway crucial for tumor proliferation and survival.

REFERENCES

1. Acs, G., Acs, P., Beckwith, S.M., Pitts, R.L., Clements, E., Wong, K., and Verma, A. (2001). Erythropoietin and erythropoietin receptor expression in human cancer. *Cancer Res* 61, 3561-3565.
2. Allen, N. (1957). Cytochrome oxidase in human brain tumours. *JNeurochem* 2, 37-44.
3. Allen, N. (1972). Oxidative metabolism of brain tumors. *Prog ExpTumor Res* 17, 192-209.
4. Argiles, J.M., and Lopez-Soriano, F.J. (1990). Why do cancer cells have such a high glycolytic rate? *MedHypotheses* 32, 151-155.
5. Argiles, J.M., and Lopez-Soriano, F.J. (1998). Host metabolism: a target in clinical oncology? *MedHypotheses* 51, 411-415.
6. Argiles, J.M., and zcon-Bieto, J. (1988). The metabolic environment of cancer. *MolCell Biochem* 81, 3-17.
7. Baggetto, L.G. (1992). Deviant energetic metabolism of glycolytic cancer cells. *Biochimie* 74, 959-974.
8. Berg, J.M., Tymoczko, J.L., and Stryer, L. (2006). *Biochemistry*, 6th edn (New York, N.Y., W. H. Freeman).
9. Bouzier, A.K., Goodwin, R., de Gannes, F.M., Valeins, H., Voisin, P., Canioni, P., and Merle, M. (1998). Compartmentation of lactate and glucose metabolism in C6 glioma cells. A ¹³c and ¹H NMR study. *JBiolChem* 273, 27162-27169.
10. Bradford, M.M. (1976). A rapid and sensitive method for the quantitation of microgram quantities of protein utilizing the principle of protein-dye binding. *Anal*

- Biochem 72, 248-254.
11. Castedo, M., Coquelle, A., Vivet, S., Vitale, I., Kauffmann, A., Dessen, P., Pequignot, M.O., Casares, N., Valent, A., Mouhamad, S., *et al.* (2006). Apoptosis regulation in tetraploid cancer cells. *EMBO J* 25, 2584-2595.
 12. Cavaliere, R., Wen, P.Y., and Schiff, D. (2007). Novel therapies for malignant gliomas. *Neurol Clin* 25, 1141-1171, x.
 13. Chiu, Y.L., and Rana, T.M. (2002). RNAi in human cells: basic structural and functional features of small interfering RNA. *Mol Cell* 10, 549-561.
 14. Colen, C.B., Seraji-Bozorgzad, N., Marples, B., Galloway, M.P., Sloan, A.E., and Mathupala, S.P. (2006). Metabolic remodeling of malignant gliomas for enhanced sensitization during radiotherapy: an in vitro study. *Neurosurgery* 59, 1313-1323; discussion 1323-1314.
 15. Dang, C.V., and Semenza, G.L. (1999). Oncogenic alterations of metabolism. *Trends BiochemSci* 24, 68-72.
 16. Dills, W.L., Jr. (1993). Nutritional and physiological consequences of tumour glycolysis. *Parasitology* 107 *Suppl*, S177-S186.
 17. Ezzell, C. (2002). Killing the messenger. Turning off RNA could thwart cancer and AIDS. *Sci Am* 287, 19, 22.
 18. Ferreira, R., Ohneda, K., Yamamoto, M., and Philipsen, S. (2005). GATA1 function, a paradigm for transcription factors in hematopoiesis. *Mol Cell Biol* 25, 1215-1227.
 19. Floridi, A., Paggi, M.G., and Fanciulli, M. (1989). Modulation of glycolysis in neuroepithelial tumors. *JNeurosurgSci* 33, 55-64.

20. Freshney, R.I. (2005). Culture of animal cells : a manual of basic technique, 5th edn (Hoboken, N.J., Wiley-Liss).
21. Gatenby, R.A., and Gillies, R.J. (2004). Why do cancers have high aerobic glycolysis? *NatRevCancer* 4, 891-899.
22. Gillies, R.J., Martinez-Zaguilan, R., Martinez, G.M., Serrano, R., and Perona, R. (1990). Tumorigenic 3T3 cells maintain an alkaline intracellular pH under physiological conditions. *ProcNatlAcadSciUSA* 87, 7414-7418.
23. Greenhouse, W.V., and Lehninger, A.L. (1976). Occurrence of the malate-aspartate shuttle in various tumor types. *Cancer Res* 36, 1392-1396.
24. Guppy, M., Leedman, P., Zu, X., and Russell, V. (2002). Contribution by different fuels and metabolic pathways to the total ATP turnover of proliferating MCF-7 breast cancer cells. *BiochemJ* 364, 309-315.
25. Halestrap, A.P., and Price, N.T. (1999). The proton-linked monocarboxylate transporter (MCT) family: structure, function and regulation. *Biochem J* 343 Pt 2, 281-299.
26. Kandel, E.R., Schwartz, J.H., and Jessell, T.M. (2000). Principles of neural science, 4th edn (New York, McGraw-Hill, Health Professions Division).
27. Kasischke, K.A., Vishwasrao, H.D., Fisher, P.J., Zipfel, W.R., and Webb, W.W. (2004). Neural activity triggers neuronal oxidative metabolism followed by astrocytic glycolysis. *Science* 305, 99-103.
28. Kaye, A.H., and Laws, E.R. (2001). Brain tumors an encyclopedic approach (London, Churchill Livingstone).
29. Kitamura, T., Tange, T., Terasawa, T., Chiba, S., Kuwaki, T., Miyagawa, K., Piao,

- Y.F., Miyazono, K., Urabe, A., and Takaku, F. (1989). Establishment and characterization of a unique human cell line that proliferates dependently on GM-CSF, IL-3, or erythropoietin. *J Cell Physiol* 140, 323-334.
30. Kleihues, P., and Sobin, L.H. (2000). World Health Organization classification of tumors. *Cancer* 88, 2887.
31. Lacroix, M., Abi-Said, D., Fournay, D.R., Gokaslan, Z.L., Shi, W., DeMonte, F., Lang, F.F., McCutcheon, I.E., Hassenbusch, S.J., Holland, E., *et al.* (2001). A multivariate analysis of 416 patients with glioblastoma multiforme: prognosis, extent of resection, and survival. *J Neurosurg* 95, 190-198.
32. Lau, N.C., and Bartel, D.P. (2003). Censors of the genome. *Sci Am* 289, 34-41.
33. Lee, A.H., and Tannock, I.F. (1998). Heterogeneity of intracellular pH and of mechanisms that regulate intracellular pH in populations of cultured cells. *Cancer Res* 58, 1901-1908.
34. Louis, D.N., and International Agency for Research on Cancer. (2007). WHO classification of tumours of the central nervous system, 4th edn (Lyon, International Agency for Research on Cancer).
35. Lowry, O.H., Berger, S.J., Carter, J.G., Chi, M.M., Manchester, J.K., Knor, J., and Pusateri, M.E. (1983). Diversity of metabolic patterns in human brain tumors: enzymes of energy metabolism and related metabolites and cofactors. *JNeurochem* 41, 994-1010.
36. Mangiardi, J.R., and Yodice, P. (1990). Metabolism of the malignant astrocytoma. *Neurosurgery* 26, 1-19.
37. Martinez, J., Patkaniowska, A., Urlaub, H., Luhrmann, R., and Tuschl, T. (2002).

- Single-stranded antisense siRNAs guide target RNA cleavage in RNAi. *Cell* 110, 563-574.
38. Marzatico, F., Curti, D., Dagani, F., Silvani, V., Gaetani, P., Butti, G., and Knerich, R. (1986). Enzymes related to energy metabolism in human gliomas. *JNeurosurgSci* 30, 129-132.
 39. Mathupala, S., and Sloan, A.A. (2009). An agarose-based cloning-ring anchoring method for isolation of viable cell clones. *Biotechniques* 46, 305-307.
 40. Mathupala, S.P., Colen, C.B., Parajuli, P., and Sloan, A.E. (2007). Lactate and malignant tumors: a therapeutic target at the end stage of glycolysis. *JBioenergBiomembr* 39, 73-77.
 41. Mathupala, S.P., Ko, Y.H., and Pedersen, P.L. (2006). Hexokinase II: cancer's double-edged sword acting as both facilitator and gatekeeper of malignancy when bound to mitochondria. *Oncogene* 25, 4777-4786.
 42. Mathupala, S.P., Parajuli, P., and Sloan, A.E. (2004). Silencing of monocarboxylate transporters via small interfering ribonucleic acid inhibits glycolysis and induces cell death in malignant glioma: an in vitro study. *Neurosurgery* 55, 1410-1419; discussion 1419.
 43. Matzke, M., and Matzke, A.J. (2003). RNAi extends its reach. *Science* 301, 1060-1061.
 44. Nolte, J., and Sundsten, J.W. (2002). *The human brain : an introduction to its functional anatomy*, 5th edn (St. Louis, Mosby).
 45. Novina, C.D., and Sharp, P.A. (2004). The RNAi revolution. *Nature* 430, 161-164.
 46. Orkin, S.H. (1992). GATA-binding transcription factors in hematopoietic cells.

- Blood 80, 575-581.
47. Orkin, S.H., and Weiss, M.J. (1999). Apoptosis. Cutting red-cell production. *Nature* 401, 433, 435-436.
 48. Pedersen, P.L. (1978). Tumor mitochondria and the bioenergetics of cancer cells. *Prog Exp Tumor Res* 22, 190-274.
 49. Pellerin, L., and Magistretti, P.J. (2004). Neuroscience. Let there be (NADH) light. *Science* 305, 50-52.
 50. Robins, H.I., Chang, S., Butowski, N., and Mehta, M. (2007). Therapeutic advances for glioblastoma multiforme: current status and future prospects. *Curr Oncol Rep* 9, 66-70.
 51. Rodriguez-Enriquez, S., and Moreno-Sanchez, R. (1998). Intermediary metabolism of fast-growth tumor cells. *ArchMedRes* 29, 1-12.
 52. Sambrook, J., and Russell, D.W. (2001). *Molecular cloning : a laboratory manual*, 3rd edn (Cold Spring Harbor, N.Y., Cold Spring Harbor Laboratory Press).
 53. Sathornsumetee, S., Rich, J.N., and Reardon, D.A. (2007). Diagnosis and treatment of high-grade astrocytoma. *Neurol Clin* 25, 1111-1139, x.
 54. Schurr, A. (2006). Lactate: the ultimate cerebral oxidative energy substrate? *JCerebBlood Flow Metab* 26, 142-152.
 55. Sharp, P.A. (1999). RNAi and double-strand RNA. *Genes Dev* 13, 139-141.
 56. Shuey, D.J., McCallus, D.E., and Giordano, T. (2002). RNAi: gene-silencing in therapeutic intervention. *Drug Discov Today* 7, 1040-1046.
 57. Stubbs, M., Bashford, C.L., and Griffiths, J.R. (2003). Understanding the tumor metabolic phenotype in the genomic era. *CurrMolMed* 3, 49-59.

58. Stubbs, M., McSheehy, P.M., and Griffiths, J.R. (1999). Causes and consequences of acidic pH in tumors: a magnetic resonance study. *AdvEnzyme Regul* 39, 13-30.
59. Tang, X.B., Liu, D.P., and Liang, C.C. (2001). Regulation of the transcription factor GATA-1 at the gene and protein level. *Cell Mol Life Sci* 58, 2008-2017.
60. Tolle, S.W., Dyson, R.D., Newburgh, R.W., and Cardenas, J.M. (1976). Pyruvate kinase isozymes in neurons, glia, neuroblastoma, and glioblastoma. *JNeurochem* 27, 1355-1360.
61. Valero, E., and Garcia-Carmona, F. (1996). Optimizing enzymatic cycling assays: spectrophotometric determination of low levels of pyruvate and L-lactate. *Anal Biochem* 239, 47-52.
62. Volk, C., Kempfski, B., and Kempfski, O.S. (1997). Inhibition of lactate export by quercetin acidifies rat glial cells in vitro. *Neurosci Lett* 223, 121-124.
63. Warburg, O. (1956). On the origin of cancer cells. *Science* 123, 309-314.
64. Wrensch, M., Minn, Y., Chew, T., Bondy, M., and Berger, M.S. (2002). Epidemiology of primary brain tumors: current concepts and review of the literature. *Neuro Oncol* 4, 278-299.
65. Zauner, A., Daugherty, W.P., Bullock, M.R., and Warner, D.S. (2002). Brain oxygenation and energy metabolism: part I-biological function and pathophysiology. *Neurosurgery* 51, 289-301.
66. Zhou, R., Vander Heiden, M.G., and Rudin, C.M. (2002). Genotoxic exposure is associated with alterations in glucose uptake and metabolism. *Cancer Res* 62, 3515-3520.

ABSTRACT**METABOLIC TARGETING OF MALIGNANT GLIOMA: MODULATION OF GLYCOLYTIC FLUX BY ERYTHROPOIETIC FACTORS**

by

TODD B. FRANCIS, M.D.**AUGUST 2010****Advisor:** Saroj Mathupala, Ph.D.**Major:** Physiology**Degree:** Doctor of Philosophy

Introduction: Malignant glioma display a highly glycolytic phenotype where the tumors flux glucose to lactic acid independent of oxygen concentration (“aerobic glycolysis”). This altered phenotype is facilitated by expression of primarily fetal enzyme isoforms in these malignant tumors. The end-product lactic acid is rapidly expelled from the cytosol by selective monocarboxylate transporters expressed on the plasma membrane. GATA response element islands are present on the promoter of glioma lactate transporter genes, and GATA-1 has been shown to be over-expressed in glioblastoma. Our long-term goal is to inhibit glioma proliferation by indirectly down-regulating GATA-1 to inhibit glycolysis (Colen et al., 2006; Mathupala et al., 2007; Mathupala et al., 2004).

Methods: We have engineered U87-MG glioblastoma tumor cell lines to either over-express (via viral promoter based vectors) or silence (using siRNA inducible vector systems) GATA-1. Cell proliferation was assessed via both MTT assay and cell cycle analysis. Luciferase based reporter gene analysis was utilized to identify regulation of lactate transporter promoter by GATA-1.

Results: Western blot analysis indicated up- and down-regulation of GATA-1 via the appropriate vector system. Up- or down-regulation of GATA-1 either enhanced or reduced the proliferative rate and the lactate transporter promoter activity.

Conclusions: Regulation of GATA-1 directly impacts glycolytic metabolic flux and proliferation of malignant glioma. Thus, small molecule drugs against GATA-1 may be used as an adjuvant therapy for metabolic targeting of malignant glioma.

KEYWORDS: Glioma, Lactate transporter, GATA

AUTOBIOGRAPHICAL STATEMENT

TODD B. FRANCIS, M.D.

EDUCATION:

- B.S. Cellular and Molecular Biology, University of Michigan, Ann Arbor, Michigan, 1998
- M.S. Basic Medical Science, Wayne State Univ., Sch. Medicine, Detroit, Michigan, 1999
- M.D. Wayne State Univ., School of Medicine. Detroit, Michigan, 2004
- Ph.D. Physiology, Wayne State University School of Medicine, Detroit, Michigan

POSTGRADUATE TRAINING:

- Internship, General Surgery, Wayne State Univ., Sch. Med./DMC, Detroit, MI, 2004-2005
- Residency - Neurosurgery, Wayne State Univ., Sch. Med., Neurological Surgery, Detroit, MI (to be completed June, 2011)
- Fellowship in Spine Surgery, Departments-Neurosurgery and Orthopedic Surgery, Cleveland Clinic Foundation, Cleveland, OH (to begin July, 2011)

AWARDS:

- 1st Place-Basic Sci., Oral Presentation: Michigan Association of Neurological Surgeons 26th Annual Mtg, Mackinac Island, MI. June, 2008 "The Metabolism of the Malignant Astrocytoma: Downregulation of Glioma Specific Lactate Transporter *in vitro* and *in vivo* Using Small Interfering Ribonucleic Acids Against Glioma Expressed Erythropoietic Factors." Francis T
- 1st Place-Oral Presentation: Michigan Association of Neurological Surgeons 27th Annual Meeting, Boyne Mountain, MI. June, 2009 "Metabolic Targeting of Malignant Glioma: Downregulation of Glioma Expressed Erythropoietic Factors via siRNA In Vitro and In Vivo." Francis, T

LICENSURE AND CERTIFICATION

Michigan License No: 4301084497 (Expiration 1/31/2012)
Board Eligible, American Board of Neurological Surgeons

GRANTS:

5R01 CA116257 (NCI/NIH) Mathupala, S.P. Ph.D. (PI) Lactate Transport as a Therapeutic Target in Glioma. Role: Resident/Graduate Student (80% Effort), 7/2006-Present

PUBLICATIONS:

1. Eltahawy HA, Rayes M, **Francis T**, Hoeprich M, Colen CB, Rengachary S: Dynamic Stabilization: Indication and Outcome. (In Preparation)
2. Rhiew RB, **Francis TB**, Mathupala SP, Barger G, Kupsky WJ, Guthikonda M, Sloan AE: Extreme Drug Resistance to BCNU in Malignant Gliomas: Survival Analysis. (In Preparation)
3. Colen CB, Shen Y, **Francis T**, Koch B, Yu P, Sloan AE, Mathupala SP: Inhibition of Lactate Efflux by Malignant Glioma Suppresses Invasiveness and Induces Tumor Necrosis. (In Preparation)
4. Rayes M, **Francis T**, Mittal S, Hornyak M, Guthikonda M, Rengachary S: Hangman's Fracture: A Historical and Biomechanical Perspective (In Preparation)
5. Rhiew RB, **Francis T**, Kupsky WJ, Guthikonda M, Sood S: Pediatric Neuroectodermal Neoplasm in Subarachnoid Space with Concurrent Craniospinal Leptomeningeal Dissemination: Case Report. (In Preparation)
6. **Francis T**, Mittal S, Shah A, Guthikonda M: Renal cell cancer metastasis to the calvarium presenting as an isolated large expansile lesion: Case report (In Preparation)
7. **Francis T**, Mittal S, Prasad M, Guthikonda M: A Rare Case of Adrenal Ganglioneuroma: Case report (In Preparation)